



Are there critical aspects in the time, energy and angular distributions of SN1987A?

Veronica Oliviero

PhD Student – University of Naples Federico II

PHYSICS MOTIVATION & THE NEW MODEL



SN1987A viewed by the James Webb Space Telescope NIRCam.

SN1987A continues to be a key object of study, as it is the only such phenomenon observed to date.

In this analysis, we analyze SN1987A data with the help of a new and more accurate modelling of the neutrino flux [Symmetry 2021, 13(10), 1851], which includes parameters describing the physics of the event.

Two main components: **accretion** and **cooling**.

$$\phi(E_\nu, t) = \phi_a(E_\nu, t) + \phi_c(E_\nu, t)$$

The associated neutrino emission was observed by three experiments: **Kamiokande-II**, **IMB** and **Baksan**. We calculated the differential interaction rate for all the experiments, also taking the background into account.

OUR ANALYSIS

The first two steps are:

- 1) Verification of the goodness of fit of the model:
Cramer test
- 2) Best-fit analysis: **Likelihood maximization**

p-values	Kamiokande-II	Baksan	IMB
Rate	Cramer: 46%	Cramer: 83%	Cramer: 44%
Energy	Cramer: 17%	Cramer: 55%	Cramer: 17 %
Angle	Cramer: 8%	N/A	Cramer: 9 %

	τ_a [s]	τ_c [s]	T_0 [MeV]	R_{ns} [km]	C_{si_0}	t_0 [s]	t_{delay} Kamiokande-II [s]	t_{delay} IMB [s]	t_{delay} Baksan [s]
Value and Uncertainty	0.51 +/- 0.15	5.5 +/- 1.3	4.5 +/- 0.5	18 +/- 7	0.02 +/- 0.02	0.10 +/- 0.06	0.00 +/- 0.02	0.00 +/- 0.02	0.00 +/- 0.03

Effects of light exposure and temperature on the quantum efficiency of PMTs for the KM3NeT Neutrino Telescope

Antonio De Benedittis - on behalf of KM3NeT Collaboration

17/06/2024



CRIS-MAC 2024



KM₃NeT Experiment

2 neutrino telescopes:

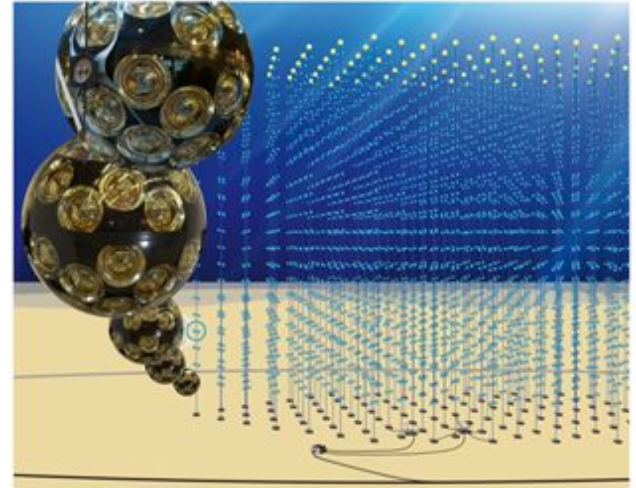
- **ARCA** off the coast of Sicily (Capo Passero) @~3.5 km of depth
- **ORCA** off the coast of France (Toulon) @~2.5 km of depth

ARCA
studies on astrophysical neutrino sources

ORCA
studies on neutrino oscillations and mass ordering

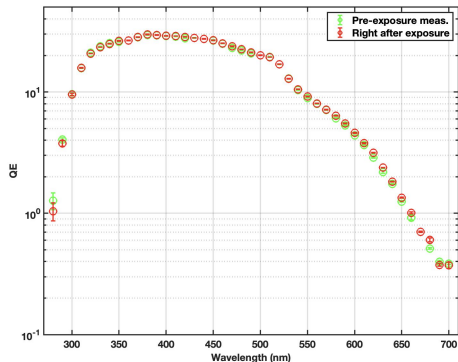
Principle

Instrumenting a large volume of water to exploit the production of Cherenkov light induced by charged particles produced by the interaction of neutrinos



Motivation of the work

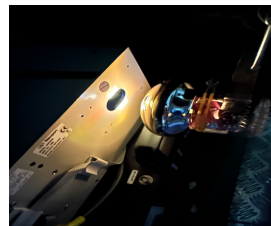
- **Photomultiplier Tubes (PMT)** are extraordinarily sensitive to low-intensity light
- **Quantum Efficiency (QE)** is crucial for accurately detecting photons and discerning the energy, direction, and characteristics of incident particles



- Very sensitive devices. They can suffer damage to the *photocathode coating*

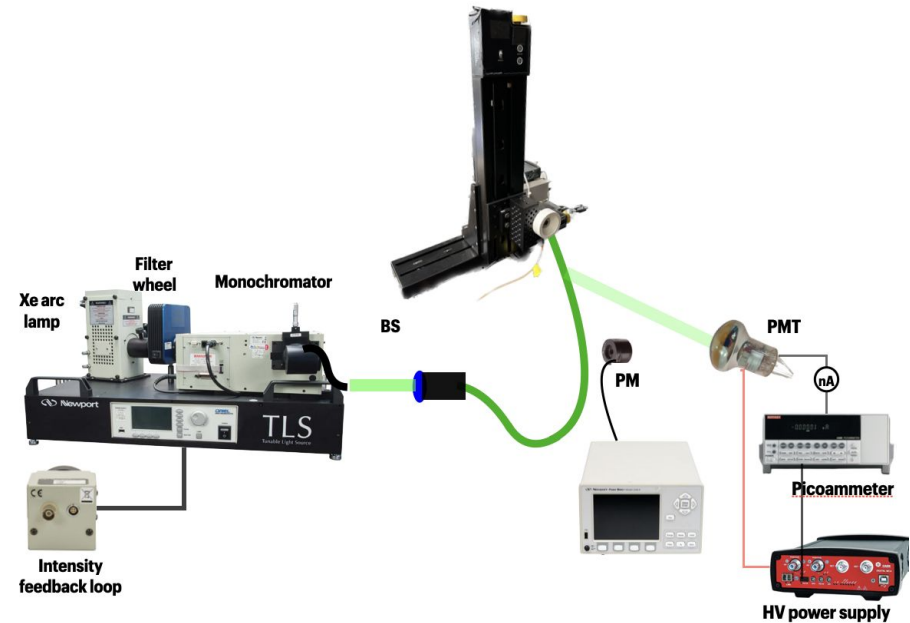


- Study on the damage threshold and recovery time of Hamamatsu **bialkali SbKCs metal-coated photomultipliers** exposed to light and thermal stress



Experimental setup

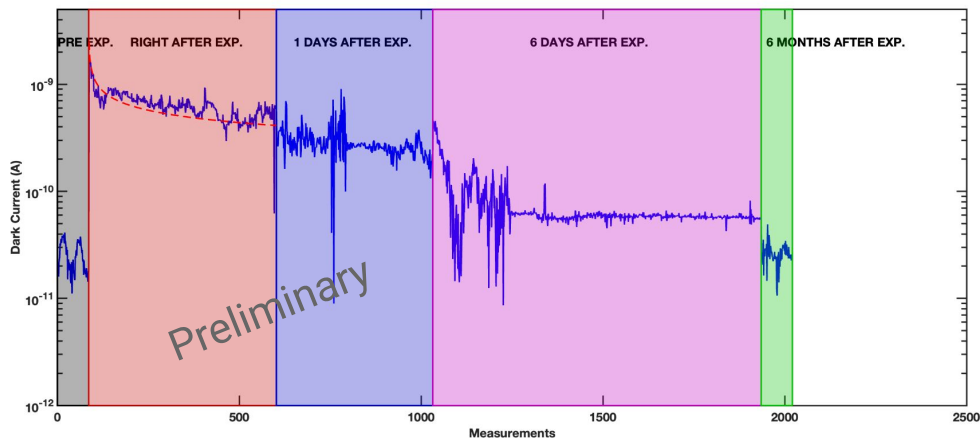
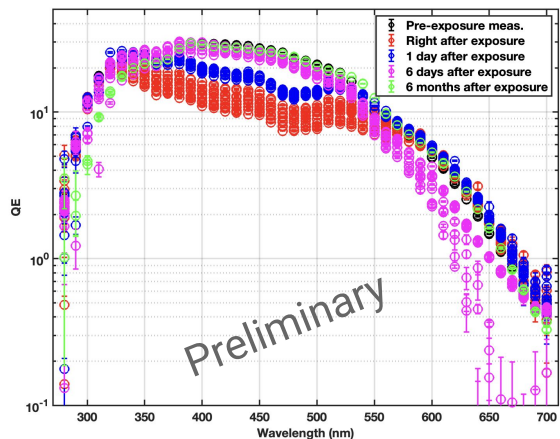
- **Newport TLS 260** tunable light source (300-watt xenon arc lamp)
- **Newport 918D-UV-OD3R** NIST calibrated power probe
- **Newport 2936 R** base for power probe connection and reading
- **Keithley 6485** picoammeter for measuring current
- **Parabolic mirror collimator** (RC02FC-F01-UV-enhanced from Thorlabs)
- Thermo-electrically cooled silicon photo-diode for active stabilization
- **LTS300C** stages from **Thorlabs** for controlling Z and X axis



Lamp exposure results

23 hours of exposure to the Xe lamp light

Lamp Irradiance = 1.22 W/cm^2
Solar Irradiance = 85.35 mW/cm^2 at $\lambda = 555 \text{ nm}$



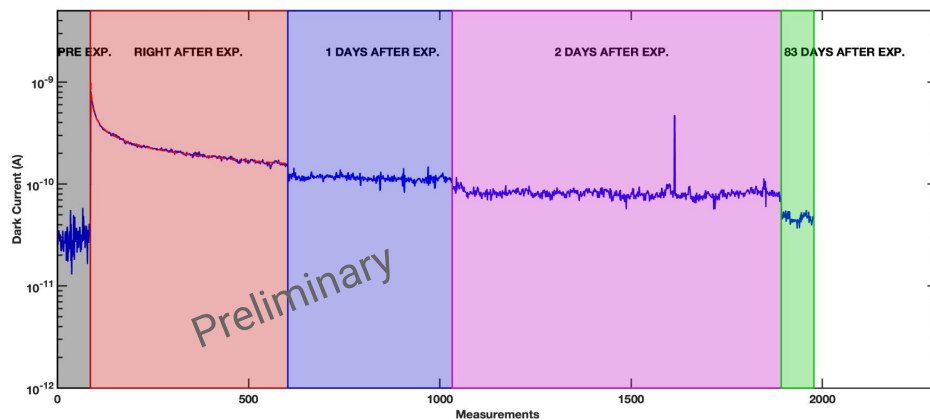
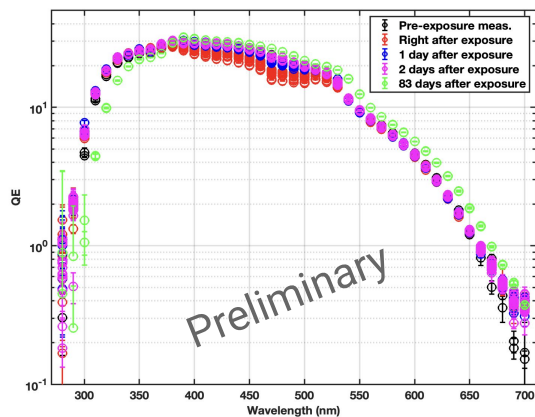
Left - **Quantum Efficiency** evolution as a function of wavelength before and after exposure. Right - **Dark Current** evolution as a function of the number of measurements

No permanent damage. Only a **temporary decrease in QE**, with a maximum reduction of about 60%, is observed in the wavelength range between 300 and 500 nm

The **Dark Current** showed alterations, gradually returning to its initial state following a **power law**

Thermal exposure results

2 days at 90° C and one day at 180° C



Left - **Quantum Efficiency** evolution as a function of wavelength before and after exposure. Right - **Dark Current** evolution as a function of the number of measurements

No permanent damage. Only a **temporary decrease in QE**, with a maximum reduction of about 15%, is observed in the wavelength range between 300 and 500 nm

The **Dark Current** showed alterations, gradually returning to its initial state following a **power law**

Summary

- Several PMTs were subjected to light and thermal stress in order to evaluate their under different conditions and to identify damage thresholds and recovery times;
- PMTs exposed to light stress were subjected to direct light from a **300-watt Xenon arc lamp** for cycles of different durations;
- PMTs exposed to thermal stress were placed in an oven for cycles of different temperatures and durations;
- In both situations:
 - No PMT showed irreversible damage (*except in one case -> See poster*);
 - a temporary decrease in **QE** was observed;
 - In these cases as well, the **dark current** follows an exponential decay law after exposure.



Combined KM3NeT/ARCA and ANTARES searches for point-like neutrino emission

Presenter: Matteo Sanguineti,
S. Alves, J. Aublin, B. Caiffi, L. Fusco, A. Heijboer, G. Illuminati,
V. Kulikovskiy, R. Muller, V. Parisi, T. van Eeden, S. Zavatarelli

on behalf of the KM3NeT and ANTARES collaborations



**Università
di Genova**



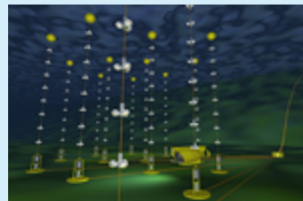
Combined point-like search

- ANTARES detector switched off in February 2022 after 15 years of data taking.
 - This analysis exploits 2007-2022 data.
- KM3NeT collaboration installs next generation of neutrino detectors in the deep sea.
 - The data from about 3 year of KM3NeT/ARCA6-8-19-21 is used in this analysis.
 - KM3NeT/ARCA operates now with 28 lines and the detector will continue to grow.

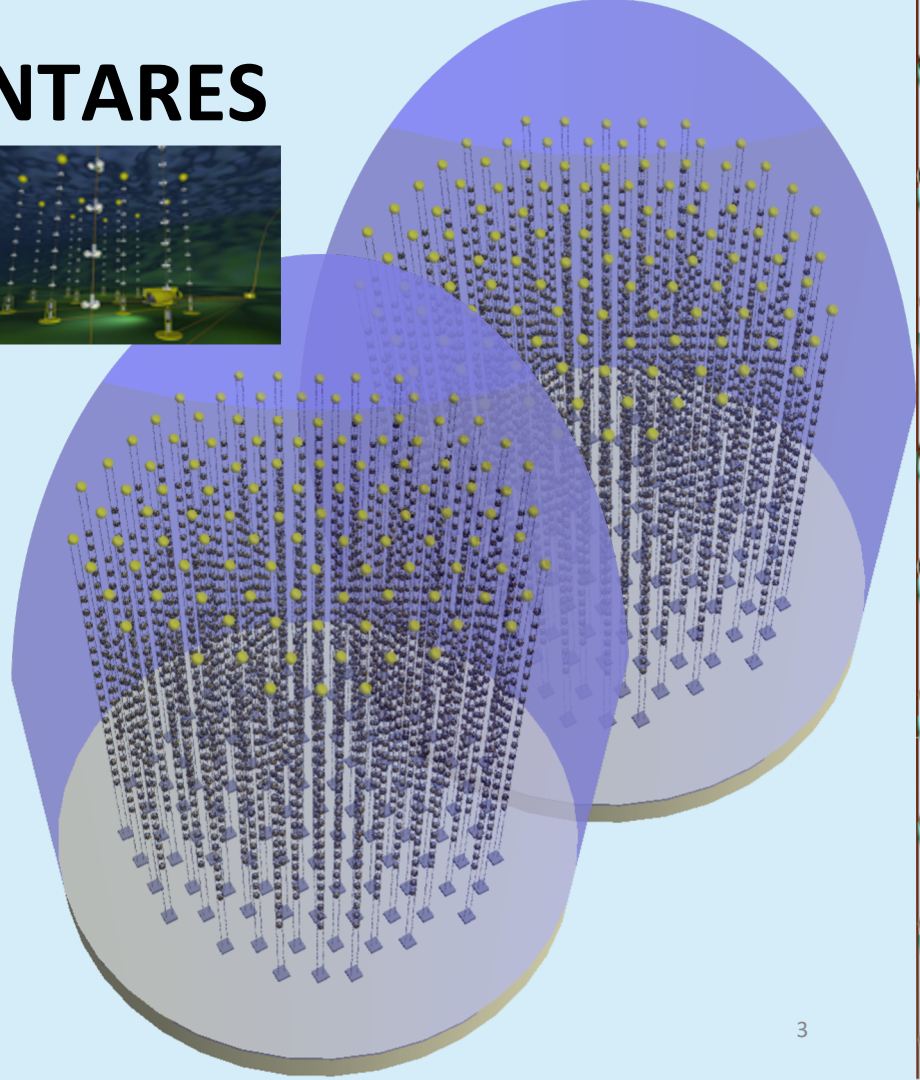


KM3NeT/ARCA and ANTARES

	ANTARES	ARCA
Effective Mass	10 Mt	1 Gt
Line length	350 m	650 m
Interline distance	70 m	90 m
OM Vertical spacing	14.5 m	36 m

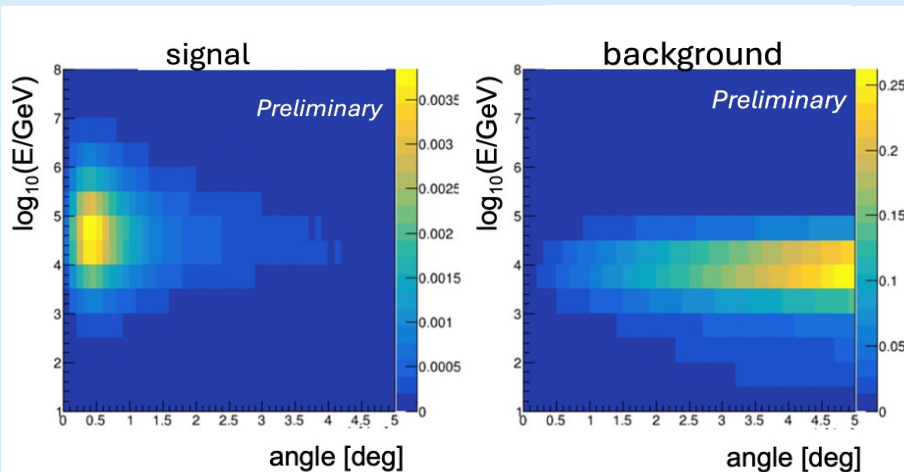


DATASET	LIVETIME [days]
ANTARES	4541
KM3NET/ARCA 6	92
KM3NET/ARCA 8	210
KM3NET/ARCA 19	53
KM3NET/ARCA 21	70

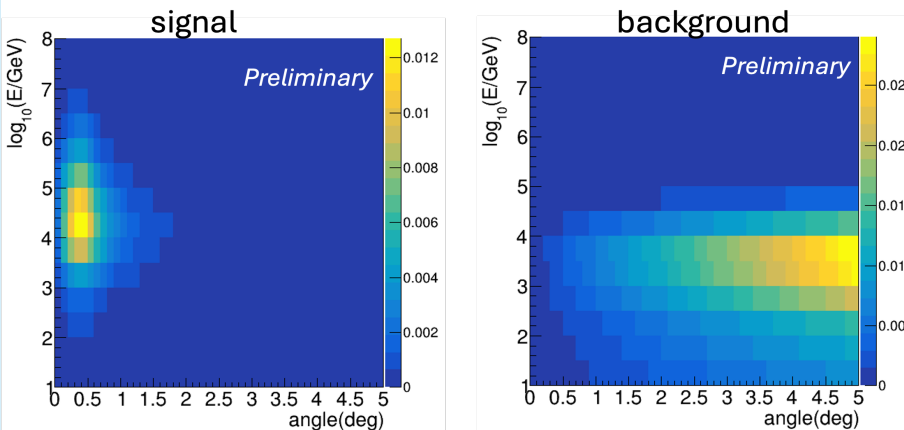


Point search analysis framework

KM3NeT/ARCA8 (210 days)
preliminary



KM3NeT/ARCA21 (70 days)
preliminary



- Data set: detector period with a particular event selection (track/showers etc).
 - Data sets do not overlap (no common events).
- For each data set:
 - Signal expectation (MC) S ,
 - Background expectation (MC, **data sampling**) B ,
 - Data/pseudo-experiment N ,

$$\log L = \sum_{bins} N_i \log(-B_i - \mu S_i) - (B_i + \mu S_i)$$

- μ signal strength (for a given default flux)

Signal estimation

$$S_i = \sum_{E_{true}} \text{rate}(\delta, E_{true}) \times f_{\alpha}(E_{true}, \alpha_{min}, \alpha_{max}) \times f_E(E_{true}, \delta, E_{rec,min}, E_{rec,max})$$

FROM
EFFECTIVE
AREA

FROM
ANGULAR
RESOLUTION

FROM
ENERGY
RESOLUTION

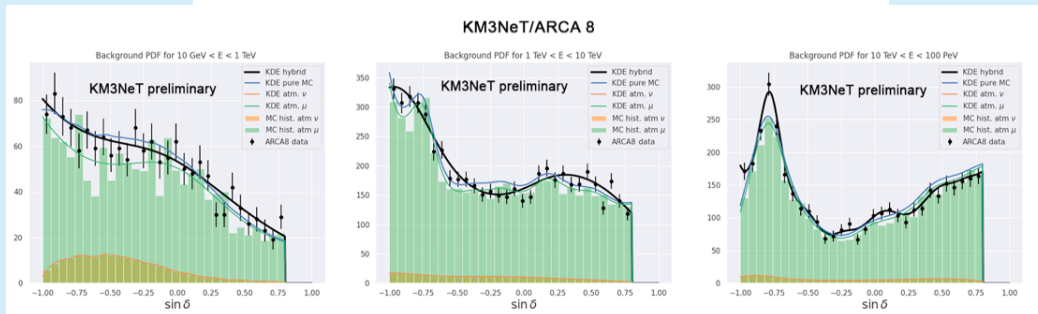
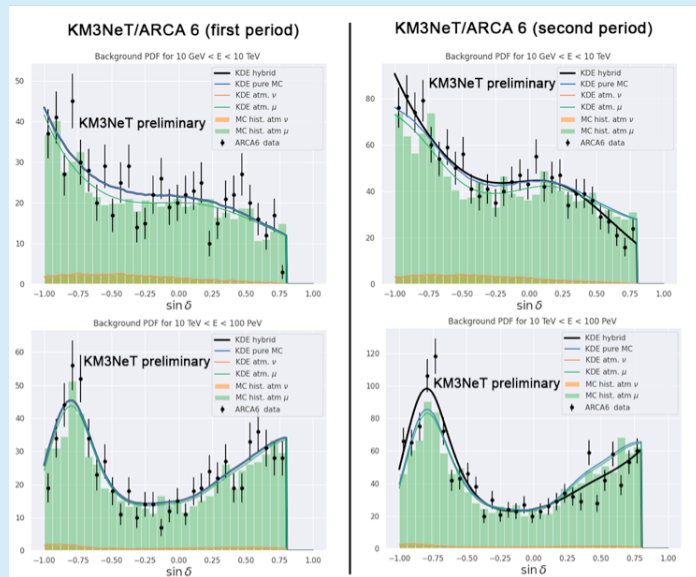
Background estimation

For ANTARES (showers),
KM3NET/ARCA 19 and
KM3NET/ARCA 21

$$B_i = n \times F(\log E) \times G(\sin \delta)$$

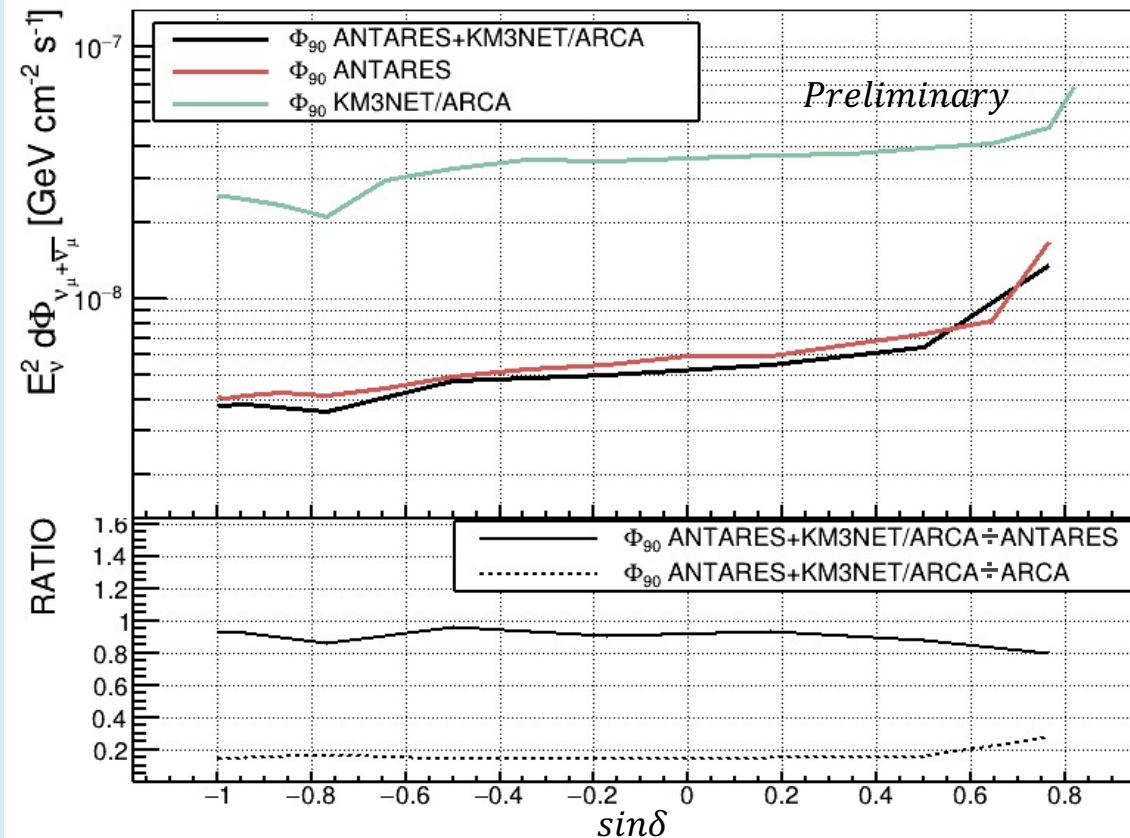
For ANTARES (tracks),
KM3NET/ARCA 6 and
KM3NET/ARCA 8

$$B_i = n \times KDE(\sin \delta, \log E)$$



Sensitivities

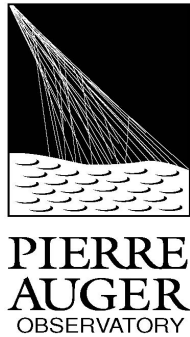
- Median Neyman upper limit for pseudo-experiments with no signal.



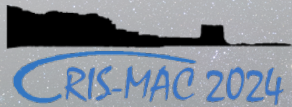
Conclusions

- The analysis framework incorporate data from the ANTARES and KM3NeT/ARCA neutrino telescope.
- Currently, ANTARES contributes most significantly, but combining with KM3NET/ARCA the performance enhances by 10%.
- The first KM3NeT/ARCA building block (consisting of 115 lines) is expected in few years. Stay tuned!

Astrophysical interpretations of the data measured at the Pierre Auger Observatory



Teresa Bister for the Pierre Auger Collaboration



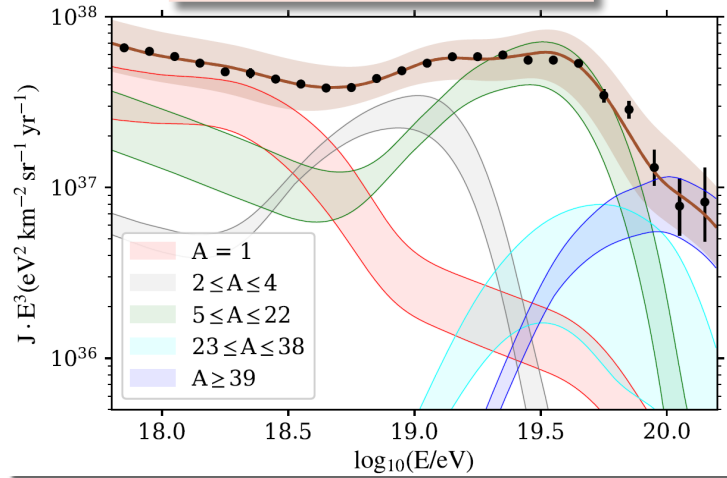
Radboud University



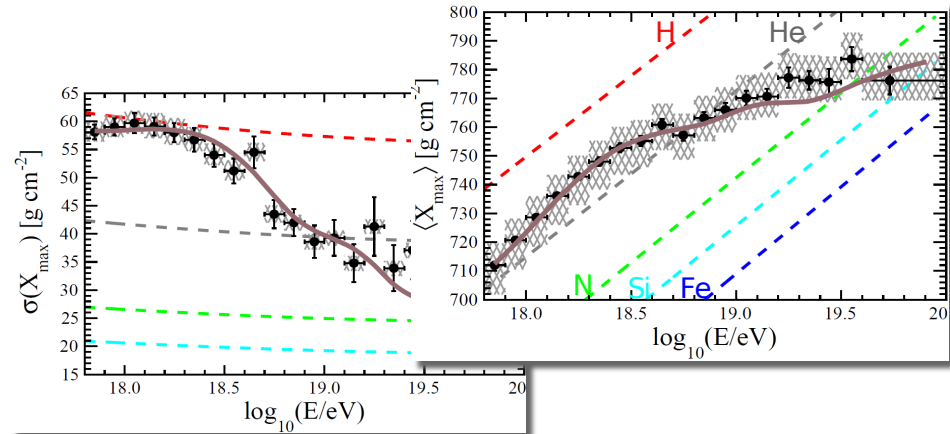
Nikhef

Ultra-high-energy cosmic ray data and interpretation

energy spectrum



mass composition

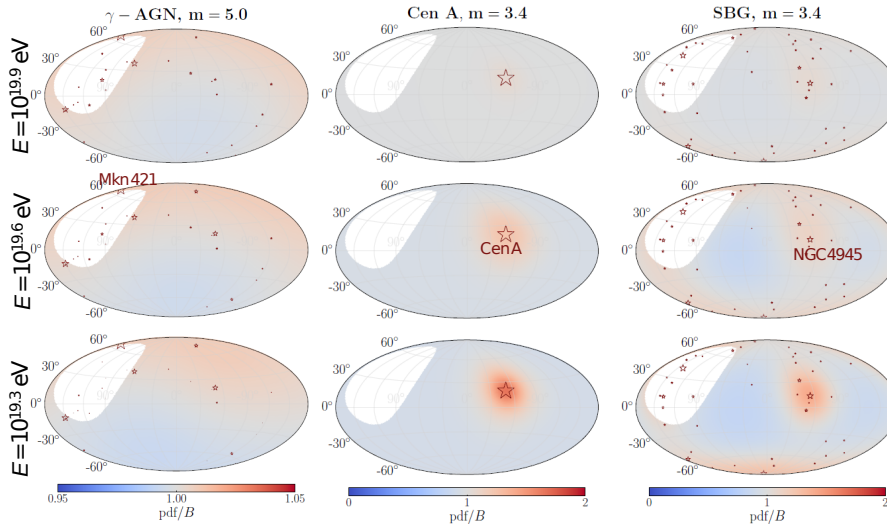


- can both be well explained by homogeneously distributed extragalactic sources!
 - need at least two populations
- can draw conclusions about injection at the source:
 - intermediate masses, hard spectrum (unlike shock acceleration expectation)

Arrival directions and magnetic fields

extensions of model:

- hard spectral index could be explained by diffusion in strong **extragalactic magnetic field**
- including **arrival directions** in the fit:
- all data well described by contribution from nearby starburst galaxies → **4.5 σ significance!**



Astrophysical interpretations of the data measured at the Pierre Auger Observatory

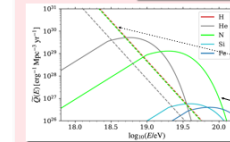
Teresa Bister for the Pierre Auger Collaboration
Radboud University Nijmegen (teresa.bister@ru.nl)
& Nationaal Instituut voor Kernfysica en Hoge-Energie Fysica (NIKHEF)

Radboud University
Nikhef

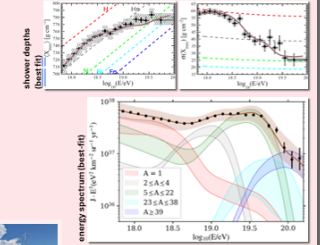


How can we explain the ultra-high-energy cosmic ray data measured at the Pierre Auger Observatory?

- explain energy spectrum and shower depth measurements [1]:
- two extragalactic populations of identical sources
- uniform distribution, evolution: $(1+z)^m$, $m \in \{0, 3.4, 5.0\}$
- Peters cycle injection: $\dot{Q}_i(E) = \dot{Q}_i \left(\frac{E}{E_0}\right)^{\gamma} \frac{1}{\exp(1 - \tau E/E_0)}$ $E \leq E_{R,cut}$
 $E > E_{R,cut}$



best-fit injection:
low-energy component:
• HeN, very soft spectrum,
• rigidity cutoff unconstrained
high-energy component:
• very hard spectrum $\gamma=0$,
• low rigidity cutoff.



Conclusions:

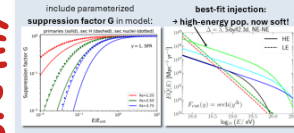
- data well described by two extragalactic populations
- ankle shaped by transition of populations
- suppression by maximum energy + propagation effects
- high-energy component with very hard injection $\gamma=0$
- similar goodness-of-fit also for same high-energy population
- protonic low-energy population + N-dominated Galactic population
- strong source evolution disfavored (also from neutrino fluxes [2])
- conclusions stable with respect to systematic uncertainties (E_{max} scale dominating)



improvement of mass uncertainty
lower with q_{max} [GeV]

What influence could the extragalactic magnetic field have?

- extragalactic magnetic field (EGMF) can suppress lower energy particles (diffusion)
- effect could explain hard best-fit spectral index at injection
- alternative: e.g. magnetic confinement in source



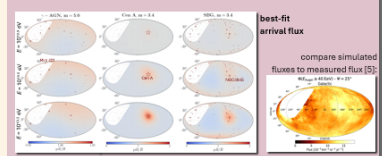
Conclusions:

- EGMF can have strong effect on injection, but only for:
- steep injection cutoff,
- & source densities $< 10^{-9}$ / Mpc³
- & very strong magnetic field strength $B_{min} = 10-200$ nG between Earth and closest sources
- then: can reach $\gamma=2$

References:
[1] The Pierre Auger Collaboration: JCAP 09 024 (2009)
[2] G. Patrino for the Pierre Auger Collaboration: JCAP 09 024 (2009)
[3] The Pierre Auger Collaboration: arXiv:2003.11311
[4] The Pierre Auger Collaboration: JCAP 01 022 (2004)
[5] The Pierre Auger Collaboration: JCAP 09 024 (2009)

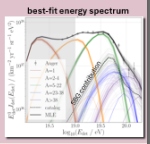
What can we learn from the arrival directions?

- extension of simple model:
- nearby source candidates [5] + homogeneous background sources (as above)
- active galactic nuclei (AGN): flux weighted by γ -ray flux + \log with $m=5$
- starburst galaxies (SBG): \log with $m=3.4$ (star formation rate)
- nearby radio galaxy Centaurus A + different bps
- fit to spectrum, shower depths & energy-dependent arrival directions

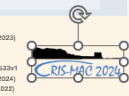


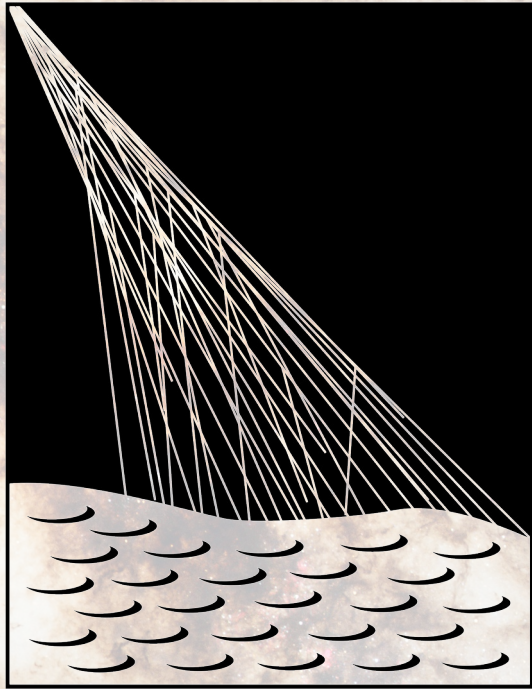
Conclusions:

- AGNs strongly disfavored
- γ -ray flux-weighting overweights Mkn 421
- SBG model describes data very well!
- 4.5 σ significance compared to model with only homogeneously distributed sources
- best fit $\sim 20\%$ from SBGs at 40 EeV
- $\sim 20^\circ$ blurring for proton at 10 EeV
- Centaurus region well described by local source at ~ 4 Mpc



Come visit my poster!



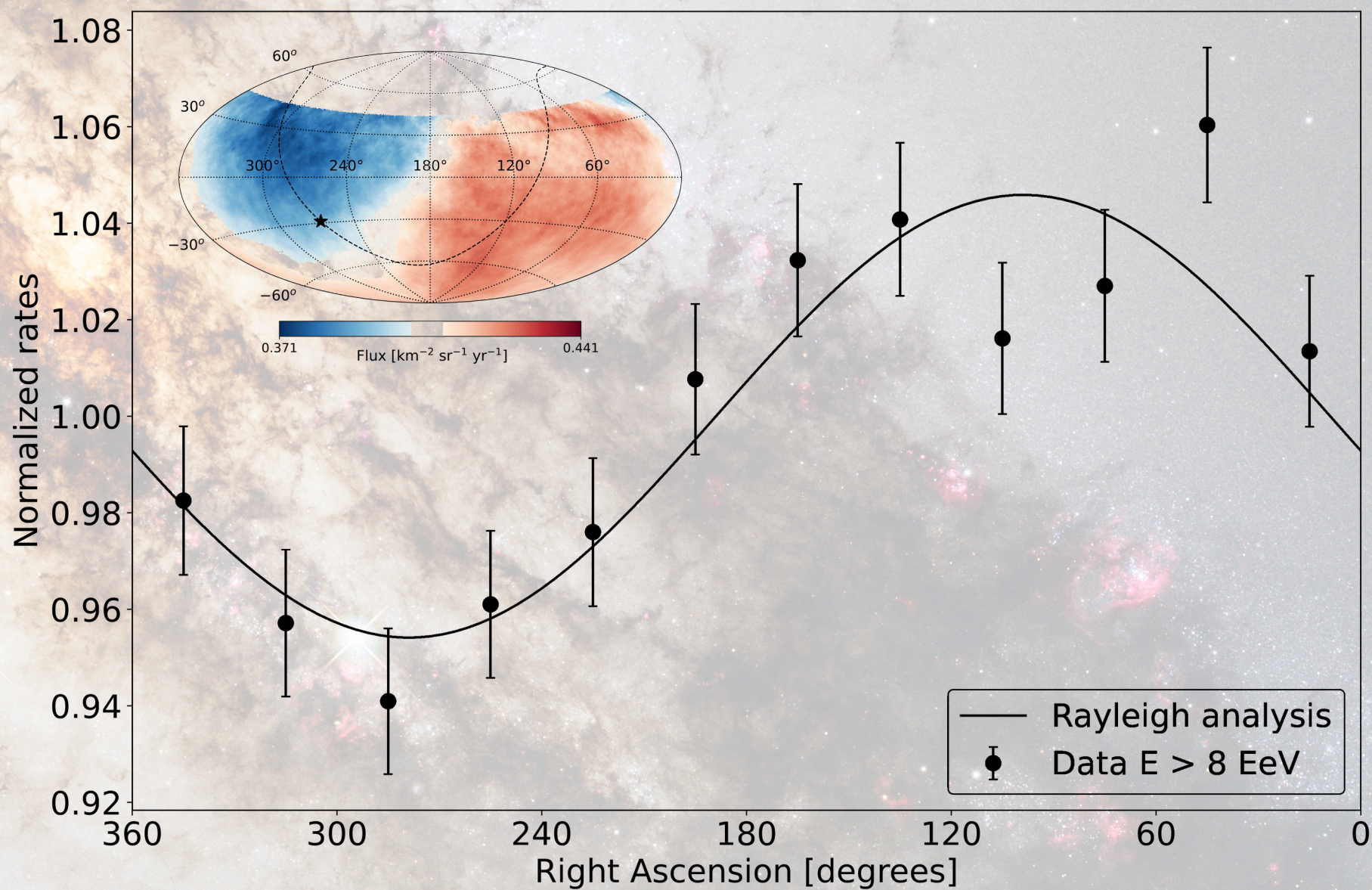


PIERRE
AUGER
OBSERVATORY

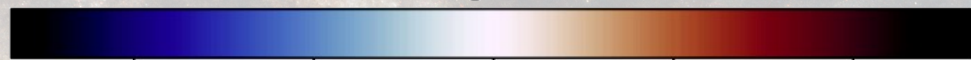
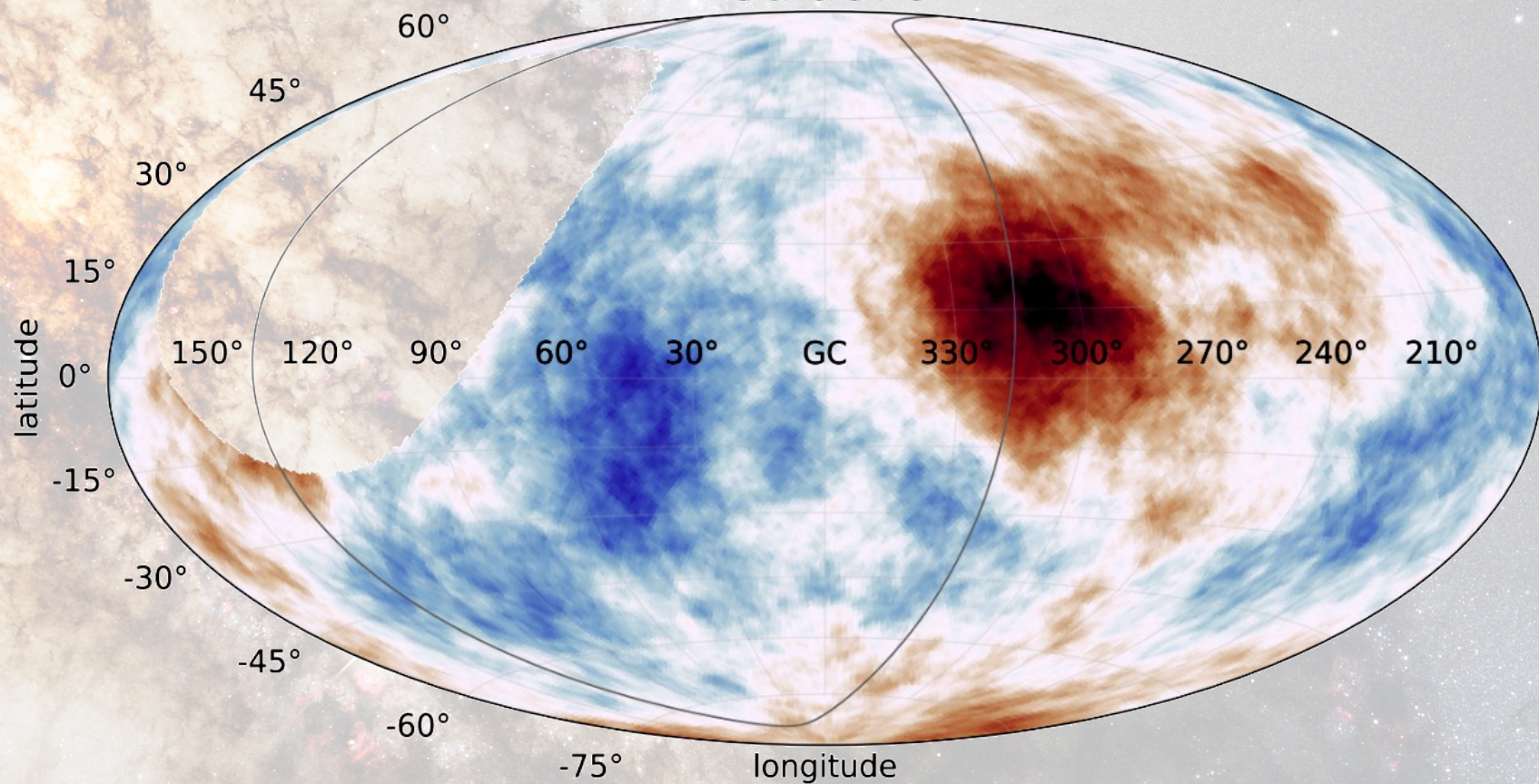
20 years of Arrival Direction Studies at the Pierre Auger Observatory

Max Stadelmaier ^{a,b,c},
for the *Pierre Auger Collaboration*

- a* *Università degli Studi di Milano UNIMI, Milano, Italy*
- b* *Istituto Nazionale di Fisica Nucleare INFN, Milano, Italy*
- c* *Karlsruhe Institut für Technologie KIT, Karlsruhe, Germany*




$\sigma(E_{\text{Auger}} \geq 38 \text{ EeV}) - \Psi = 27^\circ$
Galactic



-4 -2 0 2 4

Li & Ma significance [σ]



***See you at the
poster!***

Overview



Energy spectrum and mass composition of cosmic rays from Phase I data measured using the Pierre Auger Observatory

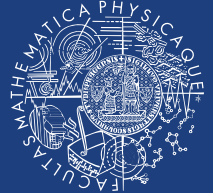
Vladimír Novotný^a for the Pierre Auger Collaboration^b

^aInstitute of Particle and Nuclear Physics, Faculty of Mathematics and Physics, Charles University, Prague, Czech Republic

^bObservatorio Pierre Auger, Av. San Martín Norte 304, 5613 Malargüe, Argentina

e-mail: spokespersons@auger.org

Full author list: https://www.auger.org/archive/authors_2024_06.html



Co-funded by
the European Union



Abstract

The Pierre Auger Observatory concluded its first phase of data taking after seventeen years of operation. The dataset collected by its surface and fluorescence detectors (FD and SD) provides us with the most precise estimates of the energy spectrum and mass composition of ultra-high energy cosmic rays yet available. We present measurements of the depth of shower maximum, the main quantity used to derive species of primary particles, determined either from the direct observation of longitudinal profiles of showers by the FD, or indirectly through the analysis of signals in the SD stations. The energy spectrum of primaries is also determined from both FD and SD measurements, where the former exhibits lower systematic uncertainty in the energy determination while the latter exploits unprecedentedly large exposure. The data for primaries with energy below 1 EeV are also available thanks to the high-elevation telescopes of FD and the denser array of SD, making measurements possible down to 6 PeV and 60 PeV, respectively.

Conclusions

In its Phase I, the Pierre Auger Observatory successfully measured, using several techniques, basic characteristics of UHECRs, namely their energy spectrum and the mass composition. The energy spectrum clearly exhibits features colloquially named the *low-energy ankle*, the *2nd knee*, the *ankle*, the *insep* and a steep suppression above 47 EeV. The mass composition seems to evolve according to Peters' cycle, being dominated by protons around 1 EeV, followed by helium nuclei around 10 EeV and the CNO group at about 50 EeV and above. Nevertheless, this inference heavily depends on predictions of high-energy interaction models and will be precised with our knowledge of these interactions.

This work was co-funded by the European Union and supported by the Czech Ministry of Education, Youth and Sports (Project FORTE - CZ.02.01.01/00/22.008/0004632).

Energy spectrum

Energy spectrum

- At the Pierre Auger Observatory, the spectrum is estimated using **six different methods** shown in Figs. 1 and 3.

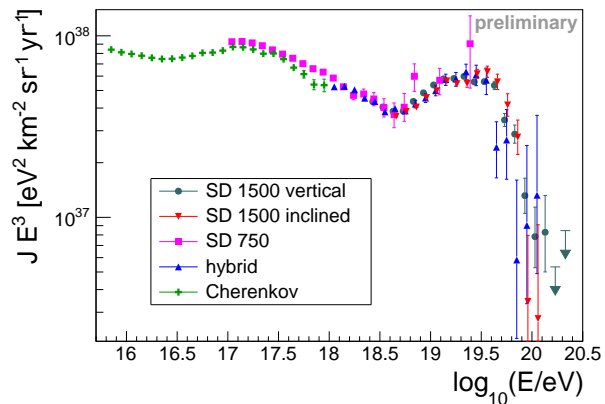


Figure 1: Energy spectrum of cosmic rays from FD (hybrid, Cherenkov) and SD data.

- Individual estimates are combined**, taking into account residual systematic differences between spectra.

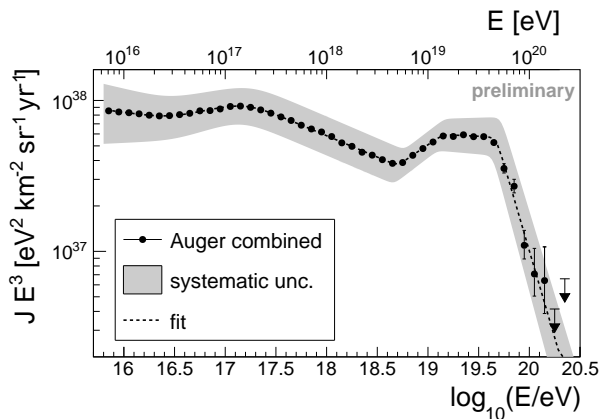


Figure 2: Combined spectrum. Common systematic uncertainty is driven by 14% uncertainty in the energy scale.

- Using the function in Eq. (1), the combined spectrum can be described by following fit values or **features**.

$$J(E) = J_0 \left(\frac{E}{10^{16} \text{ eV}} \right)^{-\gamma_0} \prod_{i=0}^4 \left[1 + \left(\frac{E}{E_{ij}} \right)^{\frac{1}{\omega_{ij}}} \right]^{(\gamma_i - \gamma_{i+1}) \omega_{ij}}, \quad j = i + 1, \quad (1)$$

normalization	$J_0 = (8.34 \pm 0.04 \pm 3.40) \times 10^{-11} \text{ km}^{-2} \text{sr}^{-1} \text{yr}^{-1} \text{eV}^{-1}$	
<i>low-energy ankle</i>	$E_{01} = (2.8 \pm 0.3 \pm 0.4) \times 10^{16} \text{ eV}$	$\gamma_0 = 3.09 \pm 0.01 \pm 0.10$
<i>2nd knee</i>	$E_{12} = (1.58 \pm 0.05 \pm 0.2) \times 10^{17} \text{ eV}$	$\gamma_1 = 2.85 \pm 0.01 \pm 0.05$
<i>ankle</i>	$E_{23} = (5.0 \pm 0.1 \pm 0.8) \times 10^{18} \text{ eV}$	$\gamma_2 = 3.283 \pm 0.002 \pm 0.10$
<i>instep</i>	$E_{34} = (1.4 \pm 0.1 \pm 0.2) \times 10^{19} \text{ eV}$	$\gamma_3 = 2.54 \pm 0.03 \pm 0.05$
<i>suppression</i>	$E_{45} = (4.7 \pm 0.3 \pm 0.6) \times 10^{19} \text{ eV}$	$\gamma_4 = 3.03 \pm 0.05 \pm 0.10$
		$\gamma_5 = 5.3 \pm 0.3 \pm 0.1$

Table 1: Parameters of the best fit of Eq. (1) to the combined spectrum. The first uncertainty is statistical and the second one systematic. Transition width parameters were fixed to $\omega_{01} = \omega_{12} = 0.25$ and $\omega_{23} = \omega_{34} = \omega_{45} = 0.05$.

- Presence of the *2nd knee* at $(2.30 \pm 0.50_{\text{stat.}} \pm 0.35_{\text{sys.}}) \times 10^{17} \text{ eV}$ was confirmed by the SD 433 m measurement.

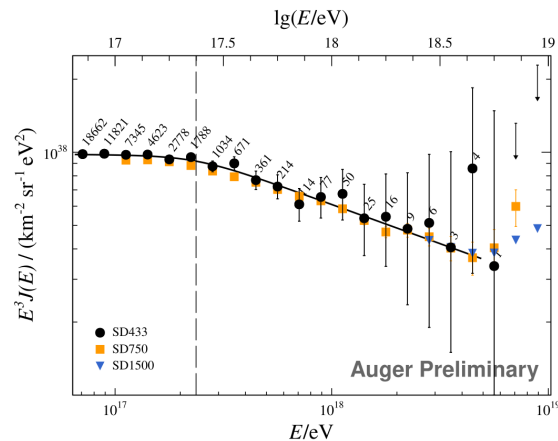


Figure 3: The *2nd knee* measured using the SD 433 m array.

- References:**

- Aab A *et al.* (The Pierre Auger Collaboration) 2020 *Phys. Rev. D* **102**(6) 062005
- Novotný V *et al.* (The Pierre Auger Collaboration) 2021 *PoS ICRC2021* 324
- Brichetto Orquera G *et al.* (The Pierre Auger Collaboration) 2023 *PoS ICRC2023* 398

Mass composition

Mass composition

► In Phase I of the Observatory measurements, we mostly rely on **the depth of shower maximum, X_{\max}** .

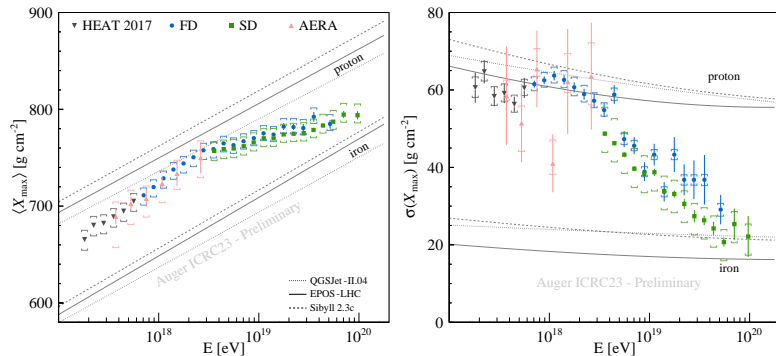


Figure 4: Average and standard dev. of X_{\max} from FD (FD, HEAT 2017), SD deep learning, and radio (AERA) data.

► Using particular high-energy interaction model, the X_{\max} moments can be translated to $\ln A$ moments.

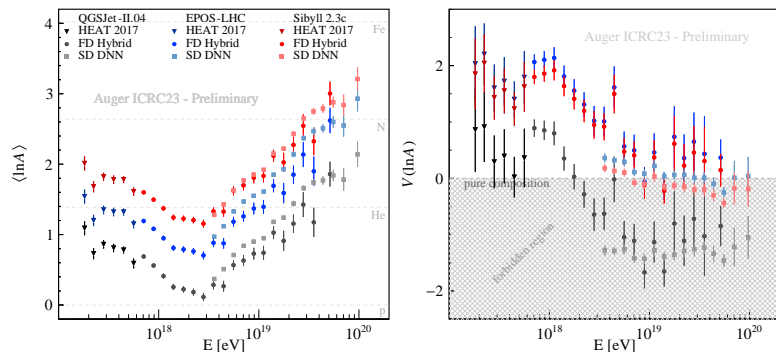


Figure 5: First two central moments of $\ln A$ calculated using contemporary models of hadronic interactions.

► **Fractions of primary mass groups** are derived by fitting model predictions to full X_{\max} distributions in energy bins.

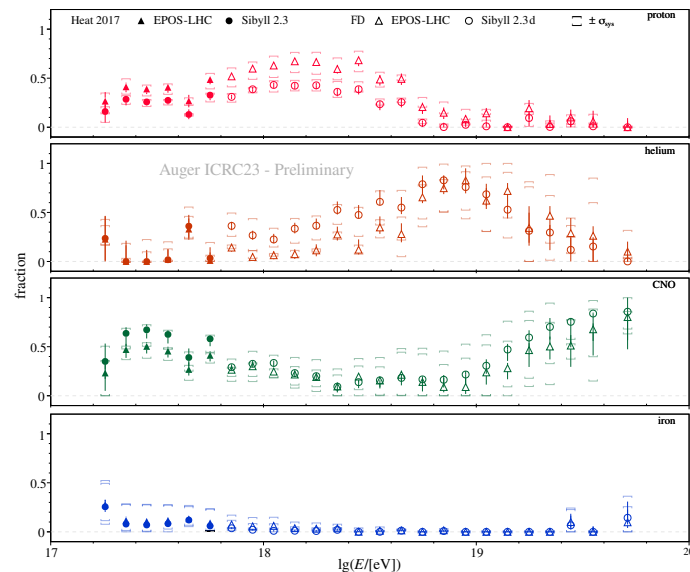


Figure 6: Primary fractions derived from the FD-measured X_{\max} distributions.

► The interpretation of X_{\max} in terms of the mass number is heavily influenced by our (lack of) knowledge of hadronic interactions at ultra-high energies.

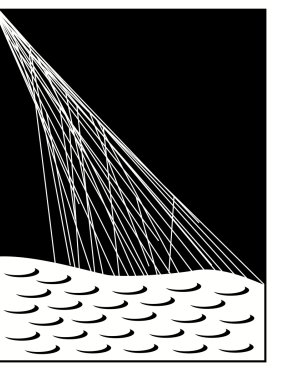
► **An unphysical region of negative $\ln A$ variances** is shown by gray band in Fig. 5. Data-points in this region stress the incompatibility between measured data and predictions of models of hadronic interactions.

► **References:**

- Fitoussi T *et al.* (The Pierre Auger Collaboration) 2023 *PoS ICRC2023* 319
- Glombitza J *et al.* (The Pierre Auger Collaboration) 2023 *PoS ICRC2023* 278
- Abdul Halim A *et al.* (The Pierre Auger Collaboration) 2024 *Phys. Rev. Lett.* **132**(2) 02100
- Mayotte E W *et al.* (The Pierre Auger Collaboration) 2023 *PoS ICRC2023* 365

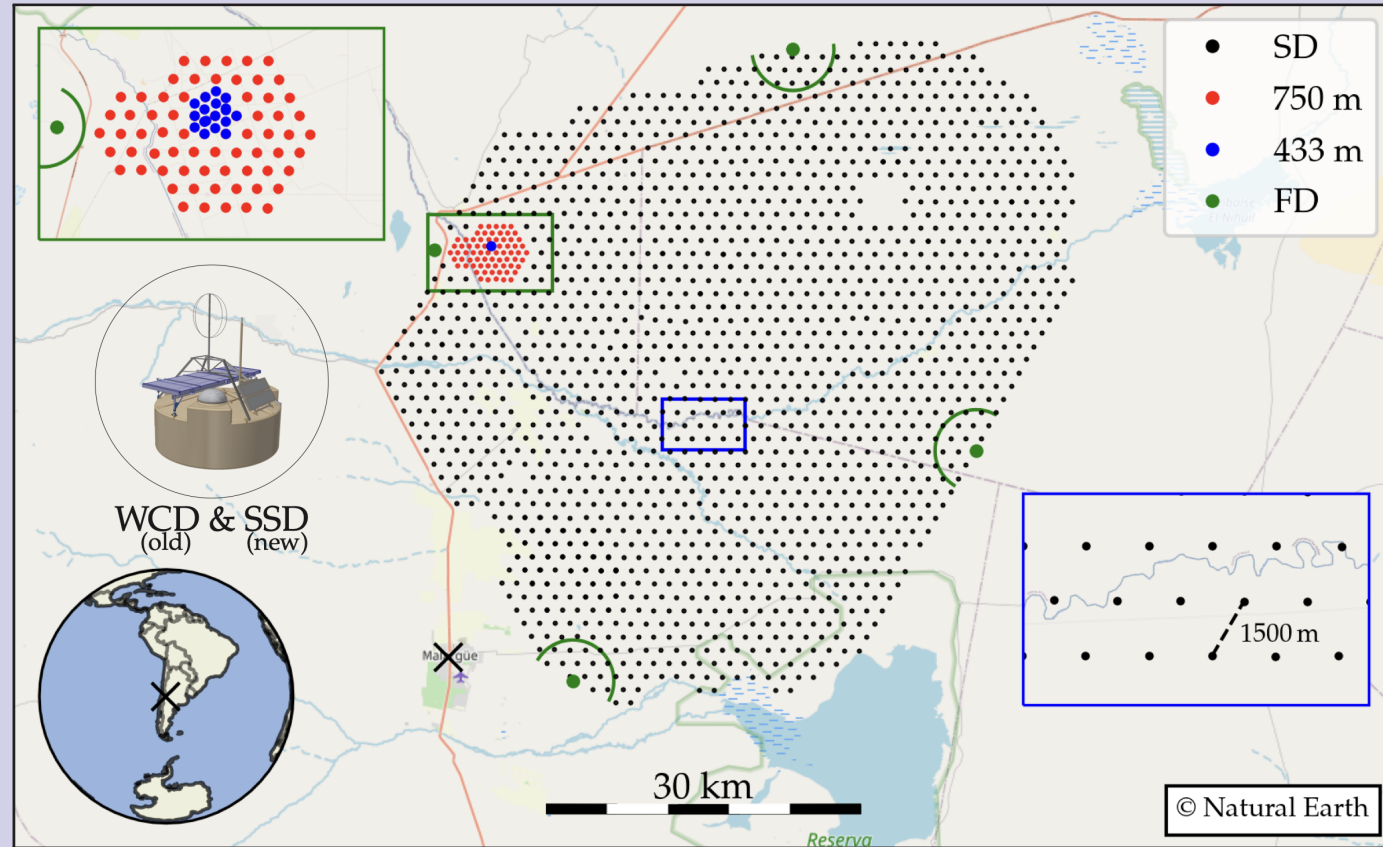
Machine Learning Applications at the Pierre Auger Observatory

Margita Kubátová* on behalf of the Pierre Auger Collaboration
*Institute of Physics of the Czech Academy of Sciences



PIERRE
AUGER
OBSERVATORY

Surface detector (SD)

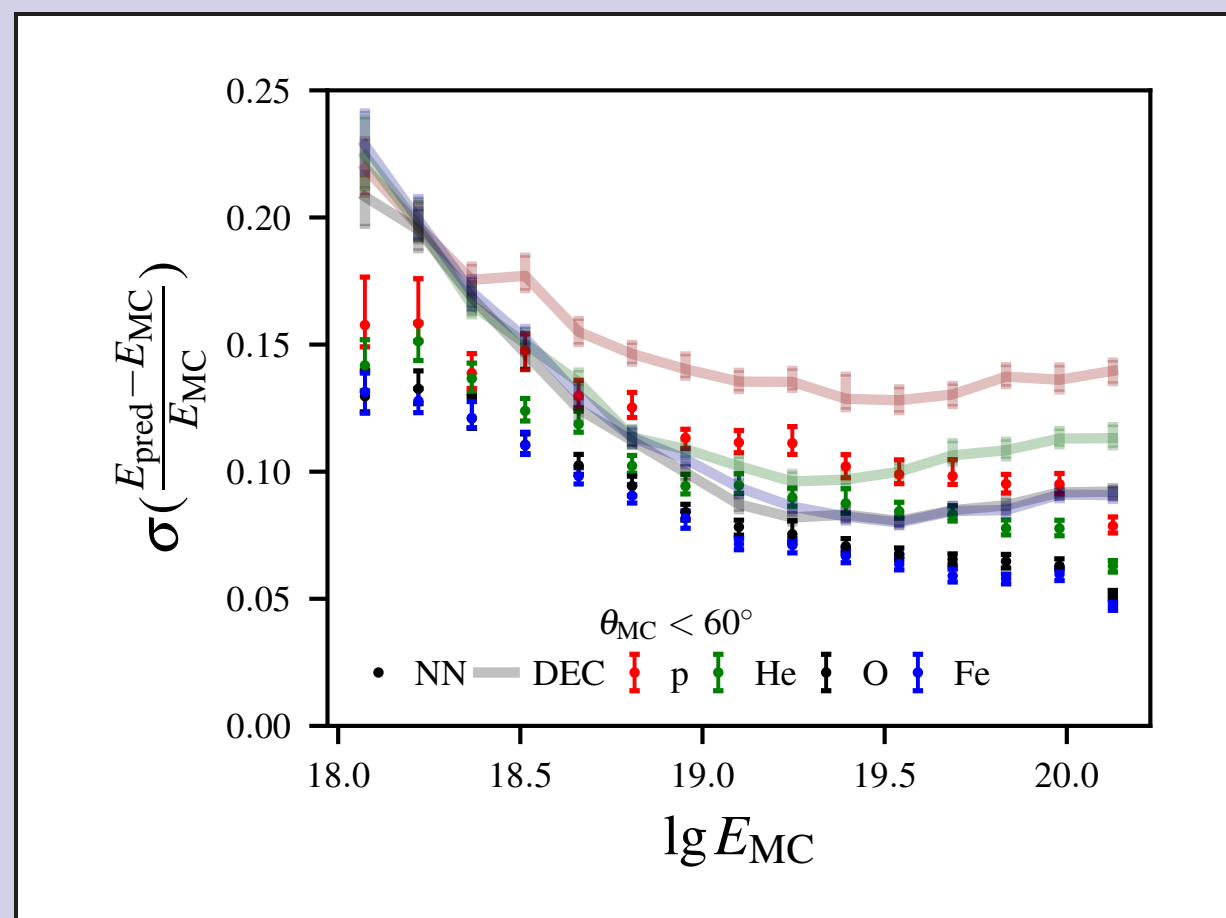
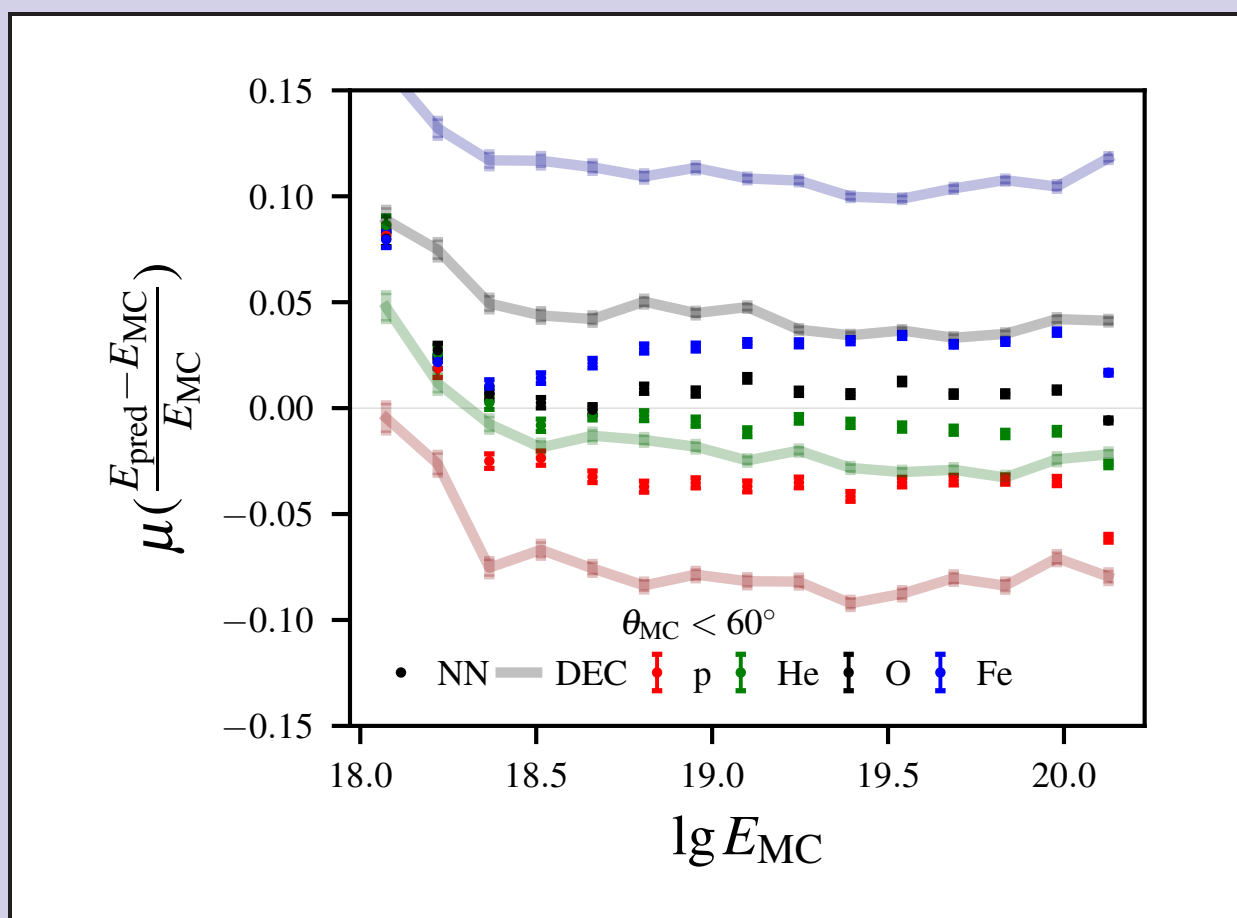


- Grid of 1660 water-Cherenkov detectors.
- AugerPrime upgrade:
 - New electronics
 - Scintillation detectors (SSD)
- ML methods use the spatial and temporal information contained in the shower footprint that is measured by the SD stations.
- Goal: Mass composition from SD.

Energy Estimator for the Surface Detector [1]

CNNs are used to reconstruct the energy of the impinging cosmic ray.

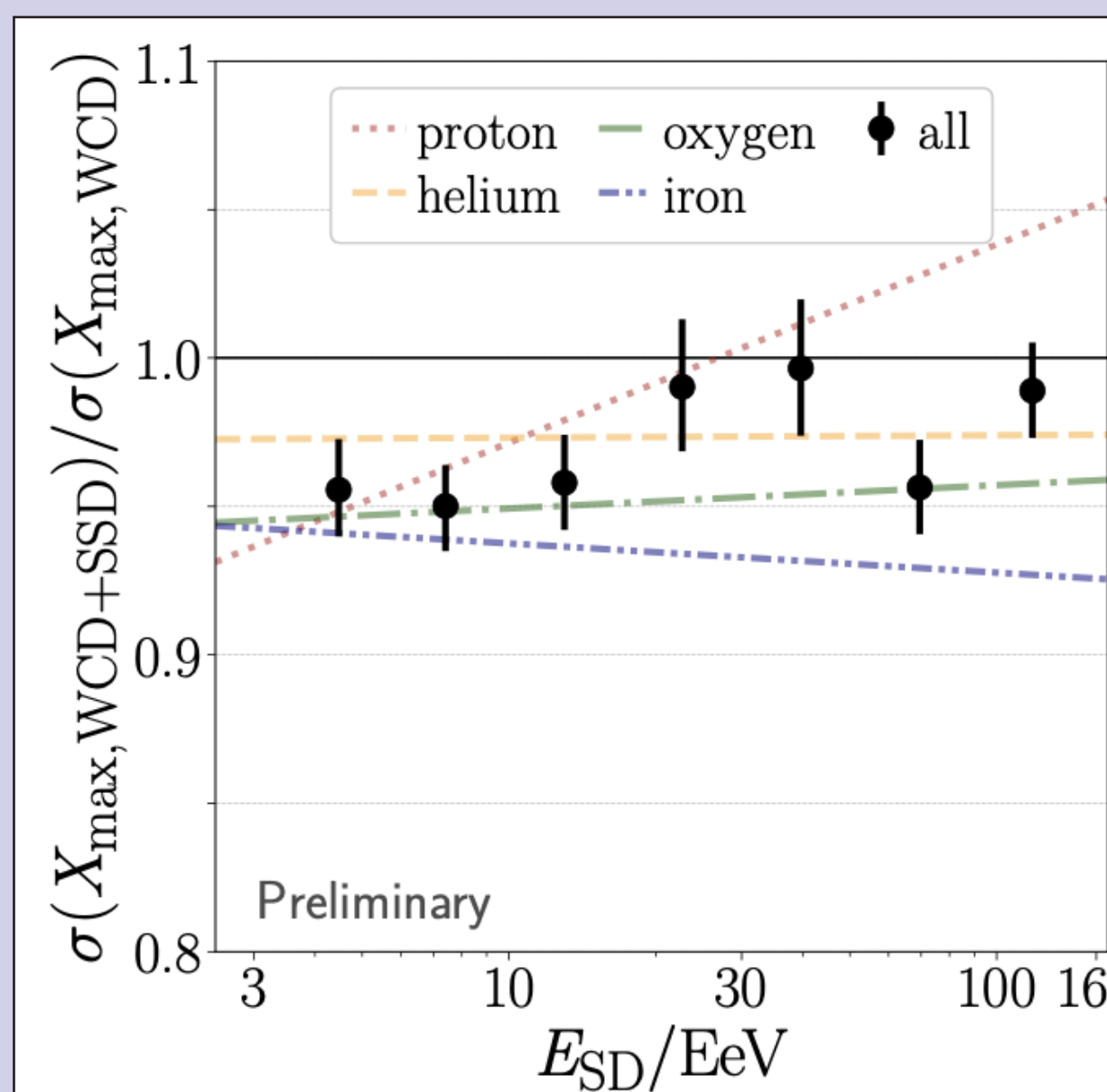
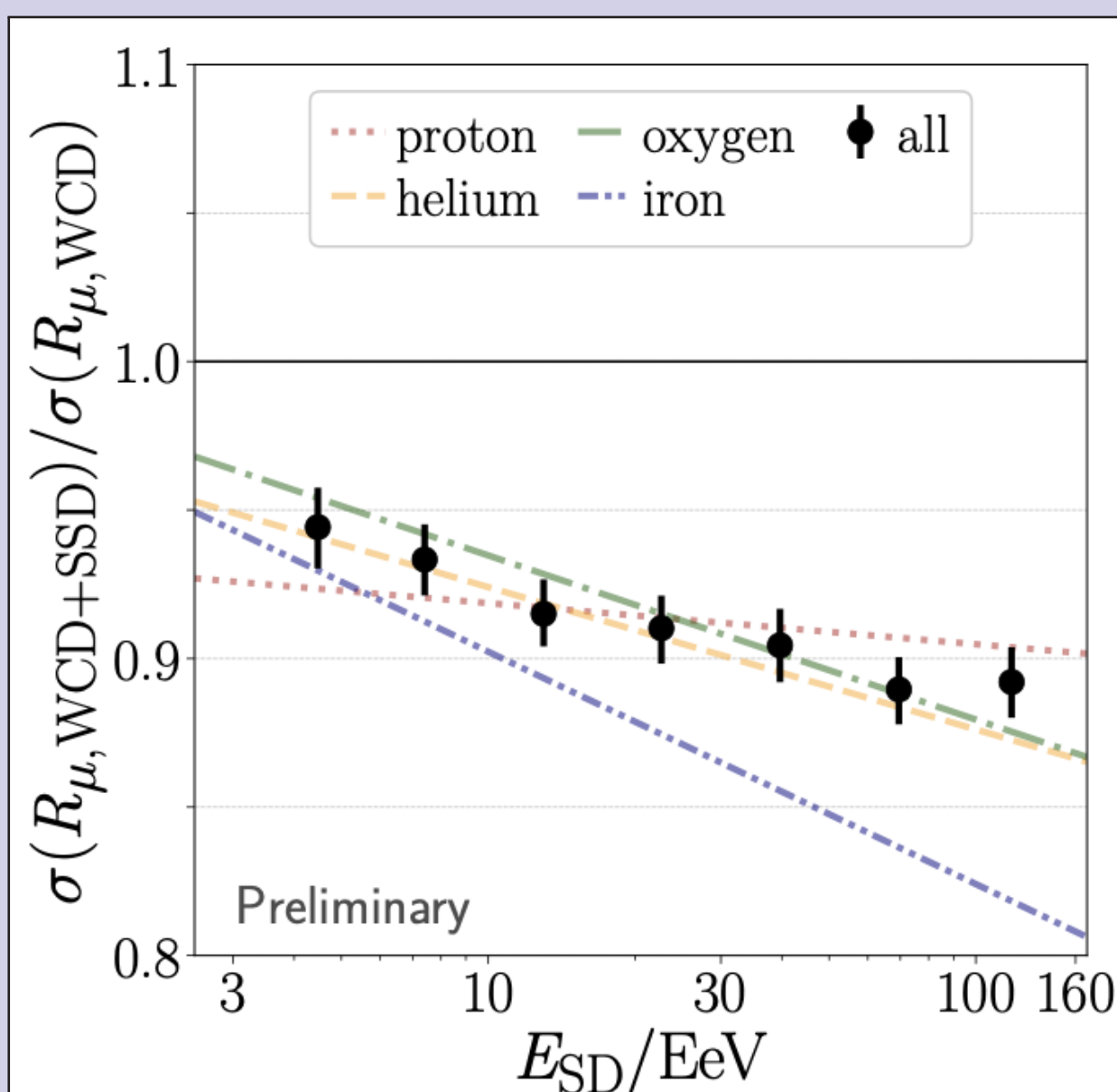
- Composition bias is reduced when compared to standard techniques.



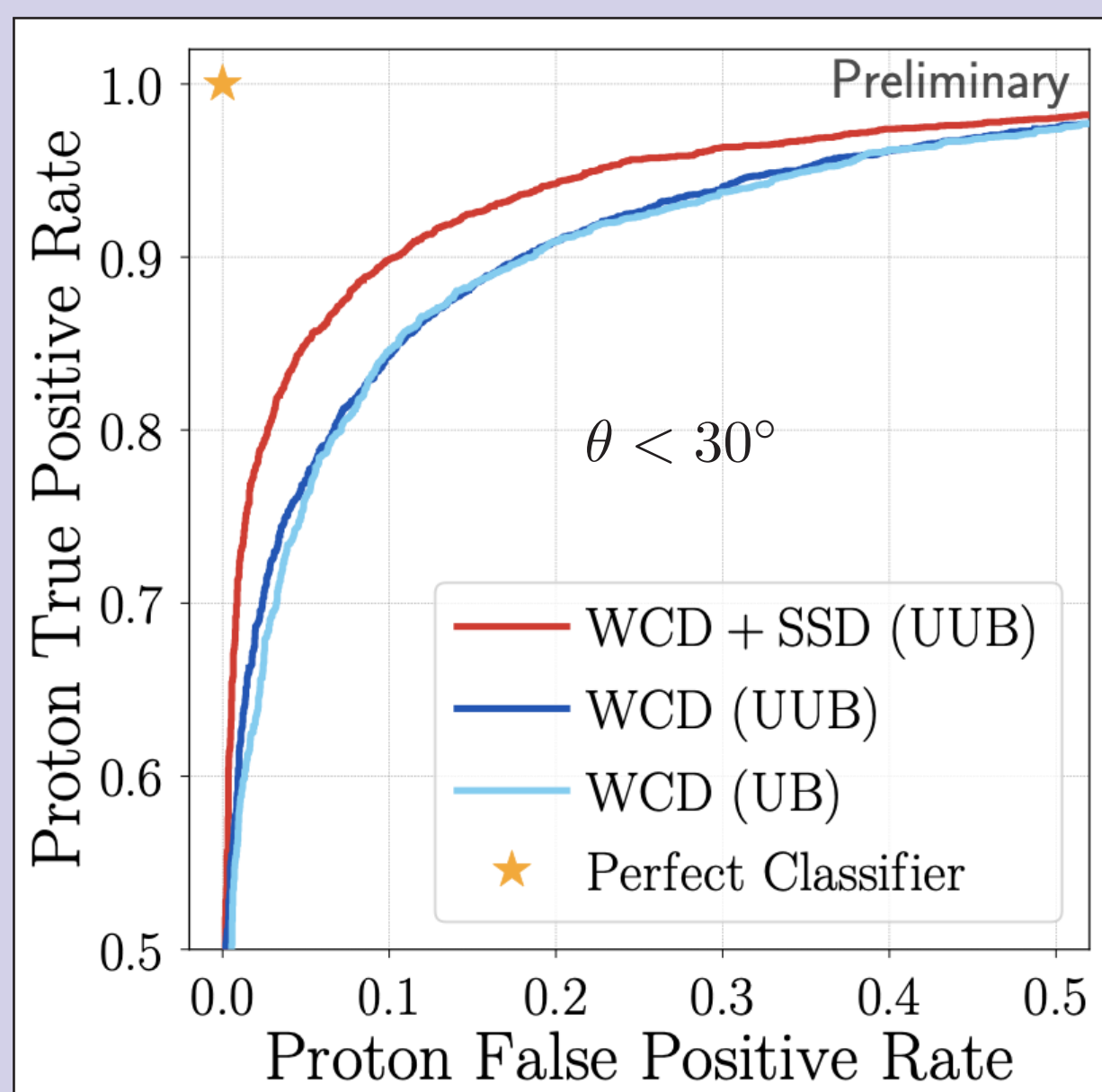
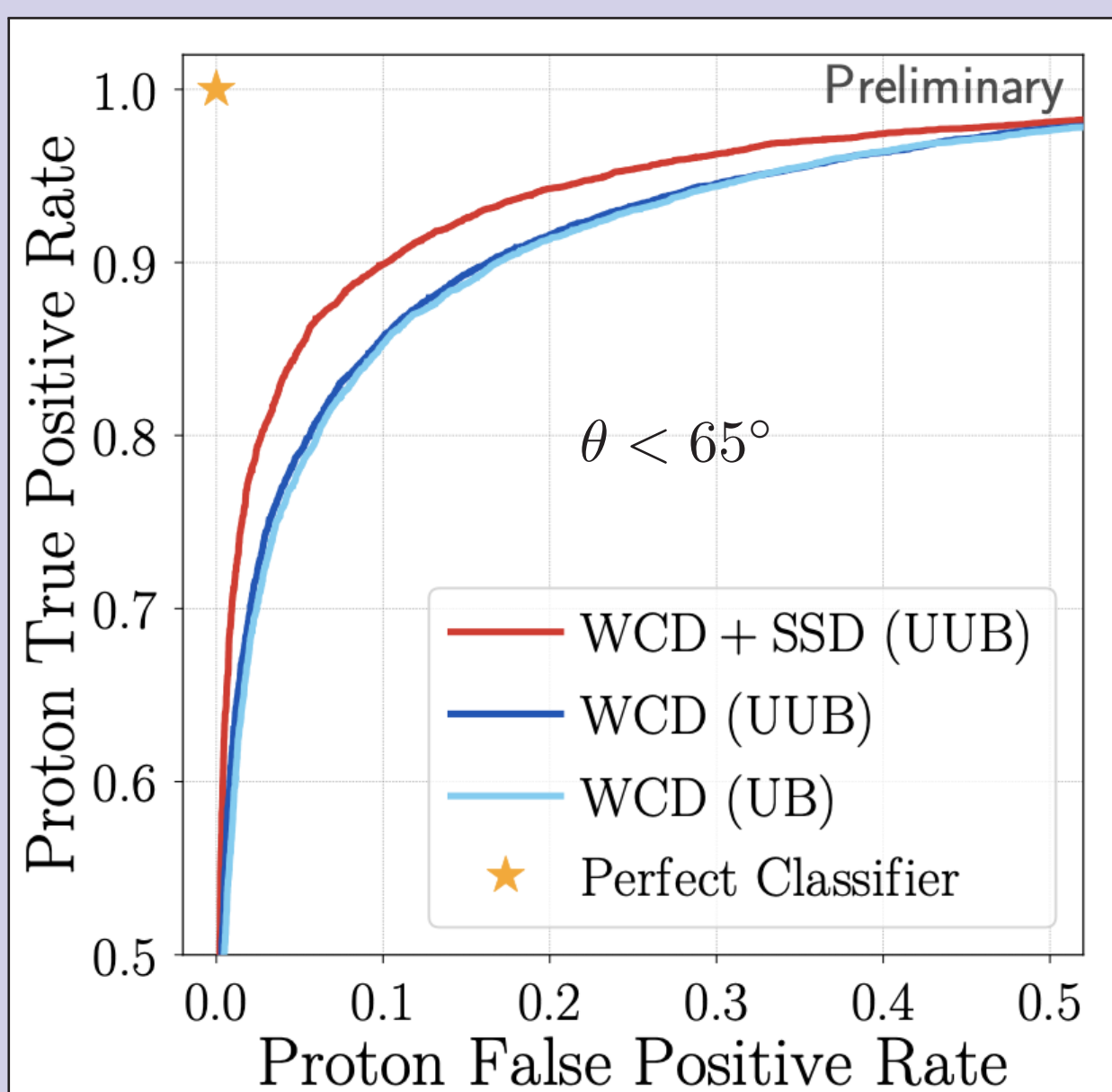
Using upgraded SD stations [3]

X_{\max} and the number of muons R_{μ} in the air shower are estimated using simulations for the upgraded stations of the SD.

- Improvement in resolution ($\sim 10\%$ for R_{μ} and $\sim 4\%$ for X_{\max}) for WCD + SSD.



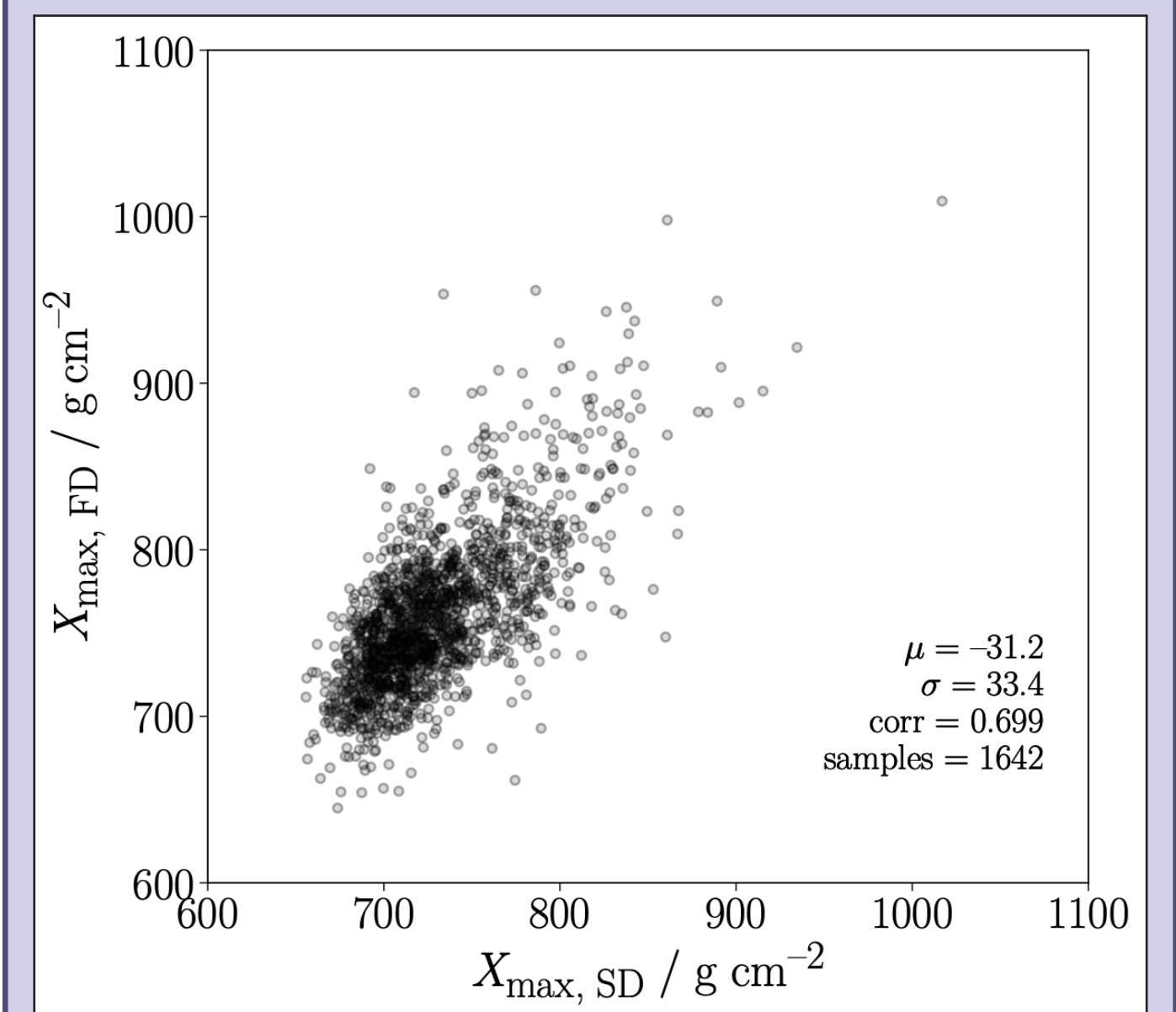
- Proton-Iron ROC curves show improvement for WCD+SSD.



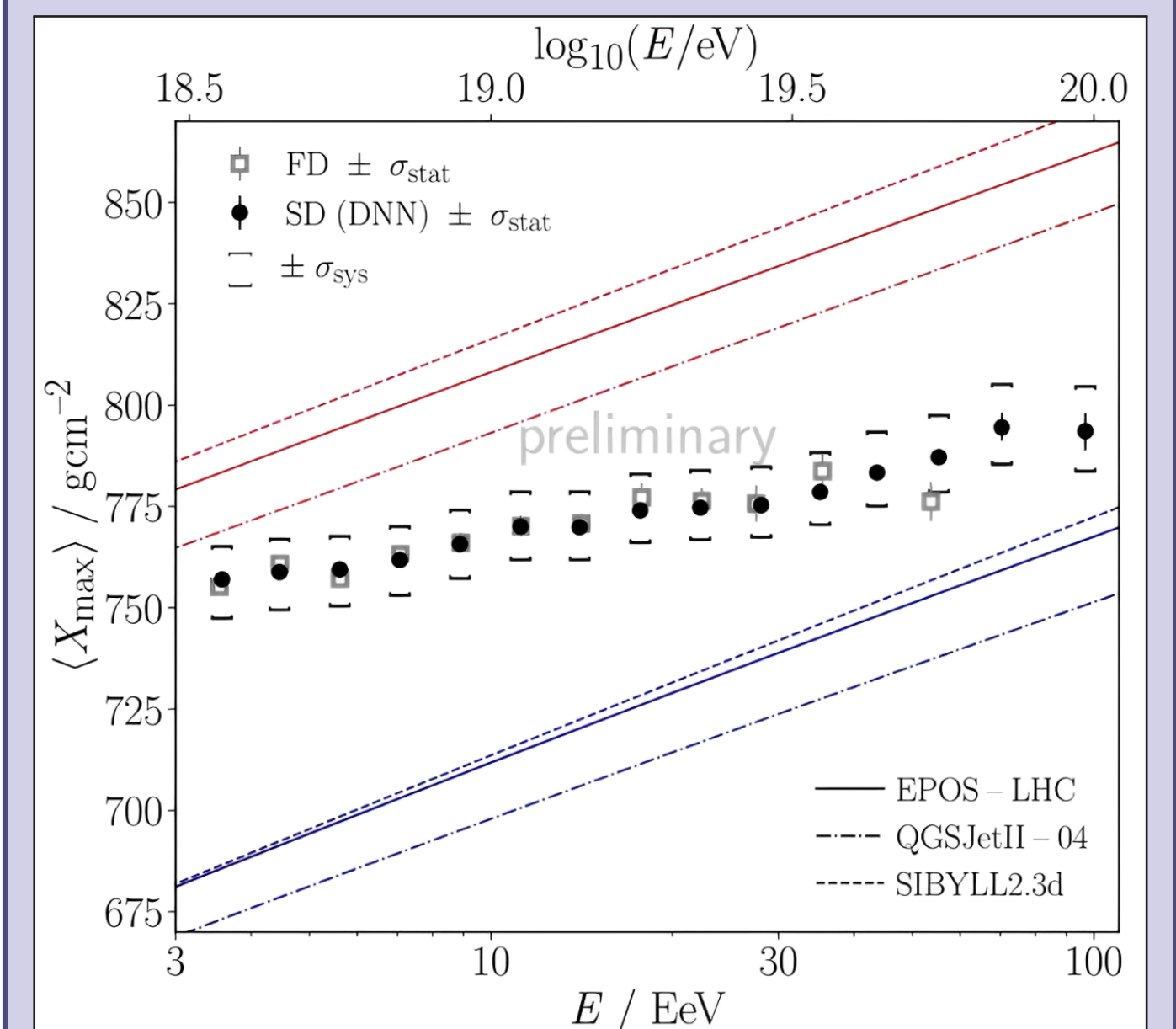
Mass Composition [2]

The depth of the maximum of air-shower profiles, X_{\max} is estimated with the combination of CNNs and LSTMs.

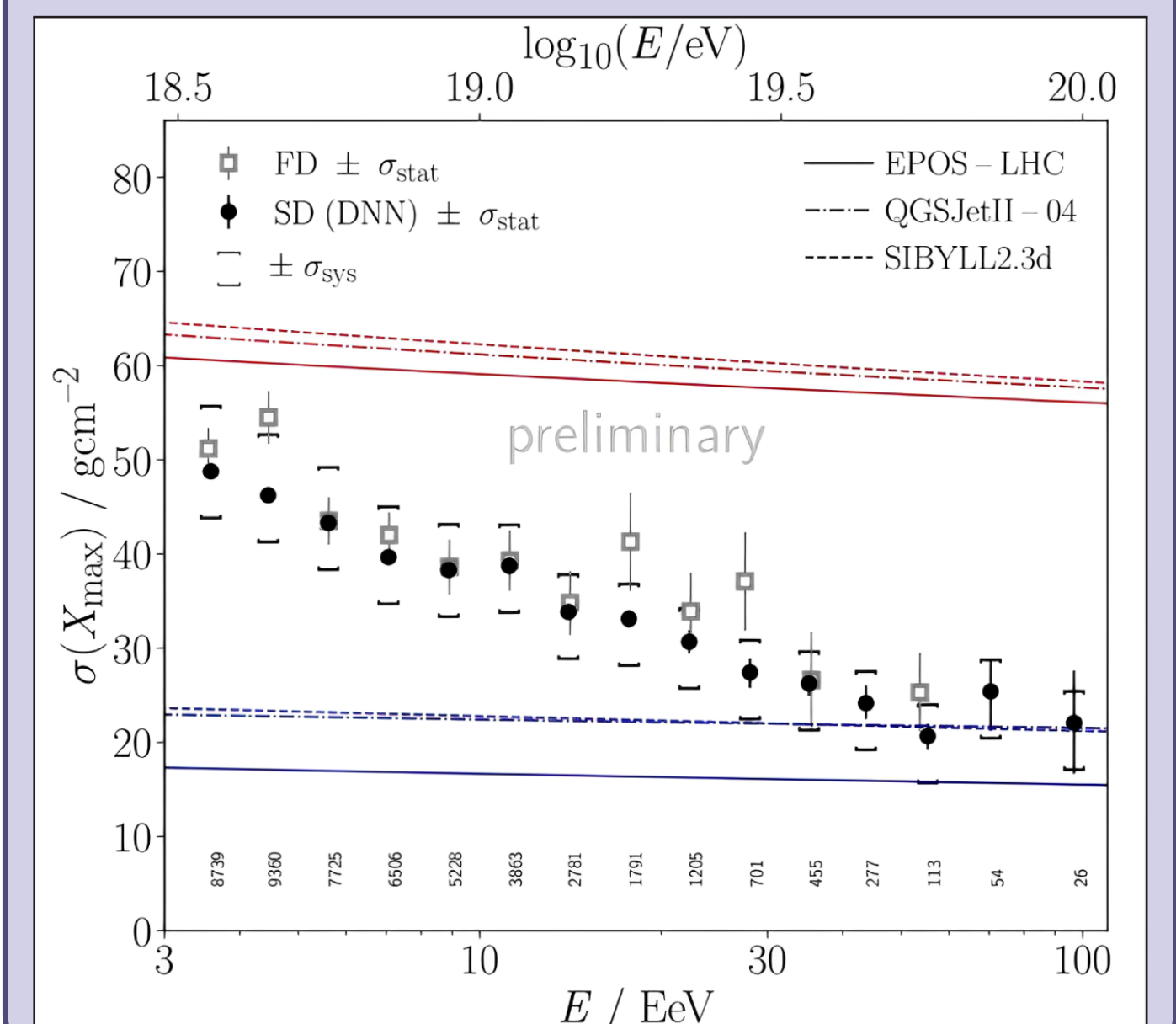
- Offset of $\sim 31 \text{ g/cm}^2$ between the SD and FD reconstruction due to mismatches between data and simulation, removed by calibration with FD data.



- There is a clear transition from a lighter to heavier composition.
- Indication for 3 breaks in the elongation rate close to the energy spectrum features.



- $\sigma(X_{\max})$ shows evolution from mixed to purer composition.



Pierre Auger Collaboration

[1] F. Ellwanger. PoS ICRC2023 (2023) 275.

[2] J. Glombitza. PoS ICRC2023 (2023) 278.

[3] N. Langner. PoS ICRC2023 (2023) 371.

Status and expected performance of the Radio Detector of the Pierre Auger Observatory

Mohit Saharan^{1,2,*}, on behalf of the Pierre Auger Collaboration^{3,**}

1: IMAPP, Radboud University, Nijmegen, the Netherlands; 2: Nikhef, Amsterdam, the Netherlands;

3: Observatorio Pierre Auger, Av. San Martín Norte 304, Malargüe, Argentina

*m.saharan@science.ru.nl, **spokespersons@auger.org

Status and expected performance of the Radio Detector of the Pierre Auger Observatory

AugerPrime upgrade

Goal: Improve mass

composition for $E > 10^{19.5}$ eV

→ Improve e/μ measurement

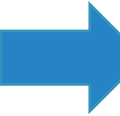
RD taking data:

Nov. 2019 to ~ May 2023

~7 stations

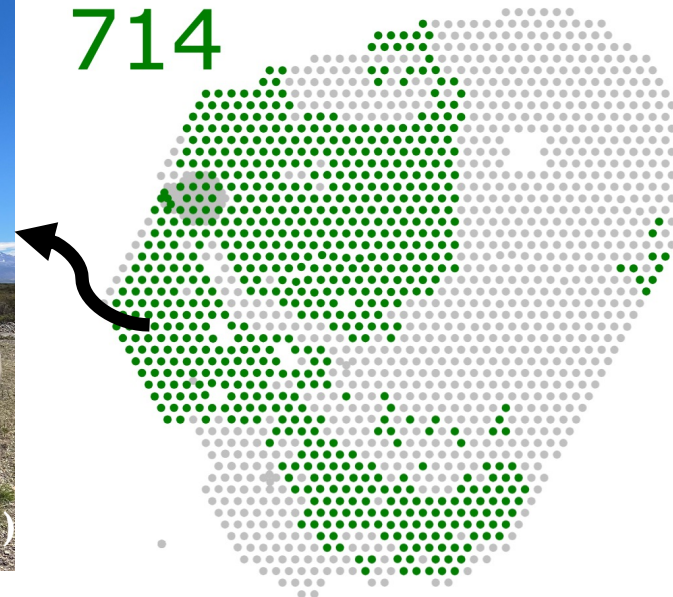


In the meantime, ...



4 June 2024

714



World's largest
radio detector
for cosmic rays



Radio Detector

RD:
EW/NS
 $\theta > 65^\circ$
30-80 MHz

New

Scintillator
Surface
Detector
 $\theta < \sim 60^\circ$

New

Particle
detectors

Old

water-
Cherenkov
detector (WCD)

Status and expected performance of the Radio Detector of the Pierre Auger Observatory

▪ **Absolute calibration:**

- Using Galactic radio emission

▪ **Relative calibration:** Partly done; ongoing

- Using drone-mounted radio emitter to map the antenna response in (θ, ϕ)

▪ **RD reconstruction:**

- Energy resolution $\sim 6\%$
- Agreement in RD and WCD reconstructed quantities

▪ **Data taking**

▪ **Reconstructed quantities consistent between data and simulations**

- We understand the RD detector design well

▪ **Expected performance for full array**

- $E > \sim 4 \text{ EeV}$: full efficiency for $\theta > 70^\circ$
- $E > 10 \text{ EeV}$: 3,000 to 4,000 events (10 years)
- Excellent p/Fe separation
- Improve mass-composition studies with high statistics for $E > 10 \text{ EeV}$

▪ **RD trigger under development:**

- RD trigger for neutral particles
- Current: only WCD trigger
- Development: hybrid WCD/RD trigger
- Improved trigger efficiency for photons
- RD-triggered events detected in field tests

More details in the poster!

POEMMA-Balloon with Radio: Mission Overview

Julia Burton for the JEM-EUSO Collaboration

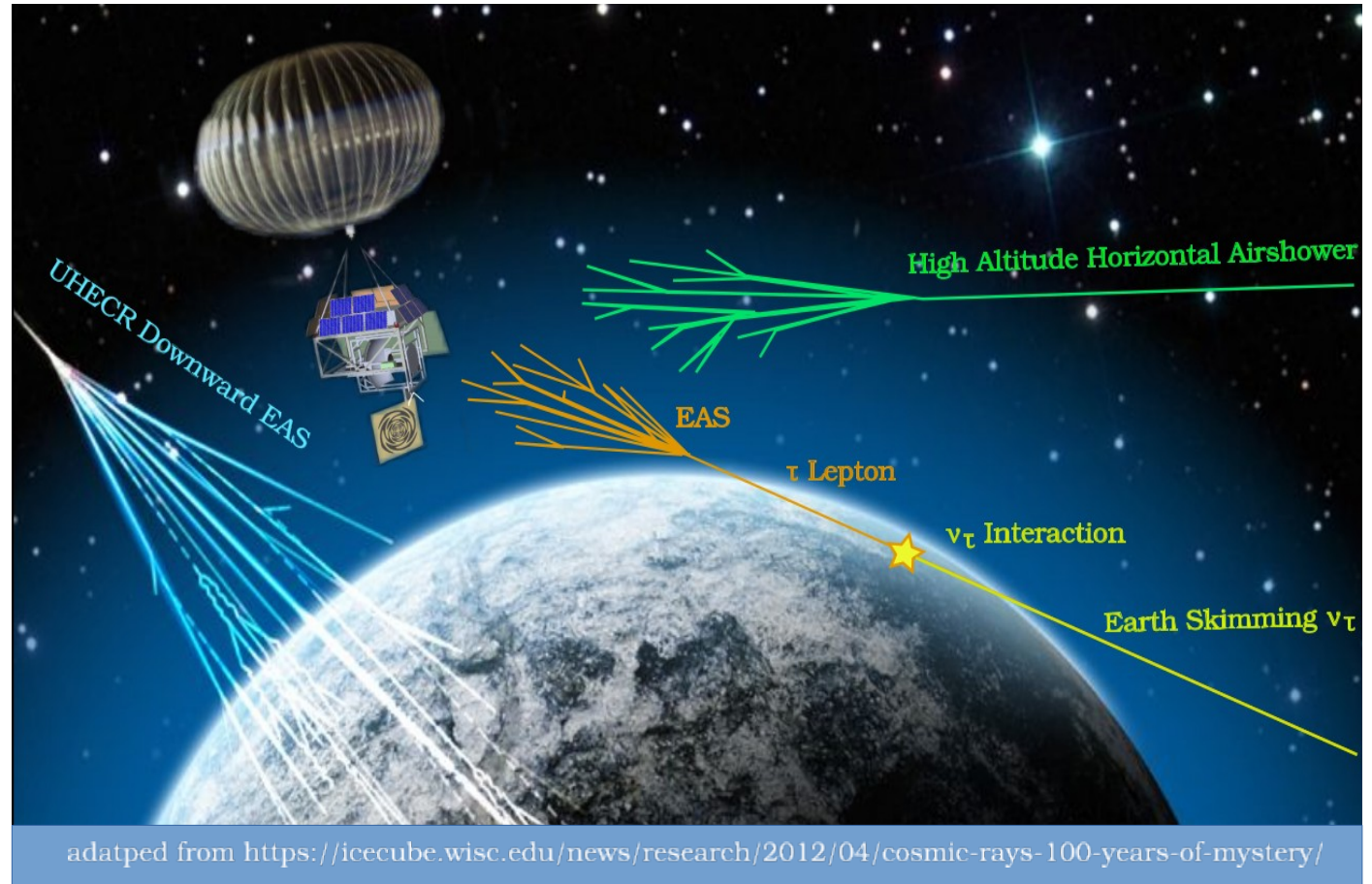
Mission Overview:

- Planned Super Pressure Balloon Mission anticipating a 2027 launch from Wanaka, NZ
- Successor Mission of Extreme Universe Space Observatory 2 (EUSO-SPB2)
- Predecessor to Probe of Extreme Multi-Messenger Astrophysics (POEMMA)



Primary Science Objectives

- Make first measurements of UHECR from above using fluorescence light emission.
- Make measurements of high-altitude horizontal air-showers (HAHAs) at various shower development stages.
- Search for Earth-skimming PeV astrophysical neutrinos.



Payload Description

1) Schmidt Optics telescope with combined focal surface:

- Fluorescence Camera
- Cherenkov Camera

2) Low Frequency Radio Instrument

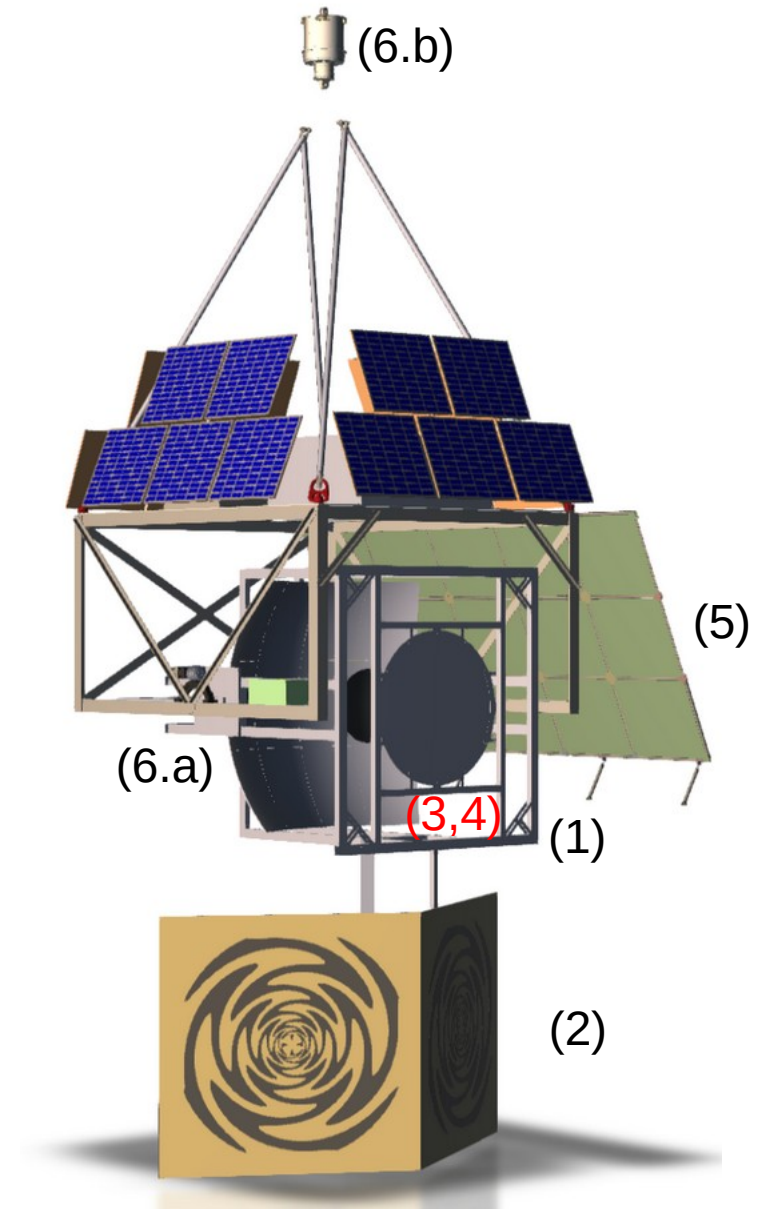
3) Infrared Camera

4) Gamma-ray/X-ray/Particle Detector

5) Solar Power System

6) Rotation Mechanism:

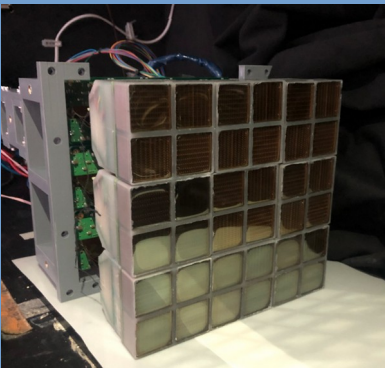
- a) Elevation: Nadir to +13 degrees above horizontal
- b) Azimuth: 360 degrees



Detectors

Fluorescence Camera

- Measures fluorescence light emission
- \gtrsim EeV energies from above
- Comprised of 4 Photo Detection Modules

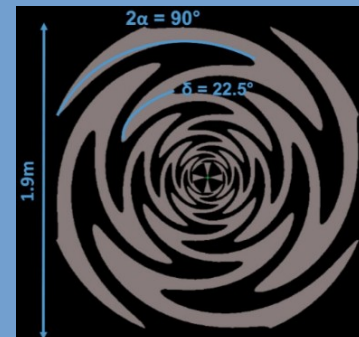


Cherenkov Camera

- Measures Cherenkov light produced by above-the-limb cosmic rays with energies of ~ 0.5 PeV
- Searches for PeV scale Earth-skimming neutrino signatures below the limb.
- 8x8 Silicon Photo-Multiplier array

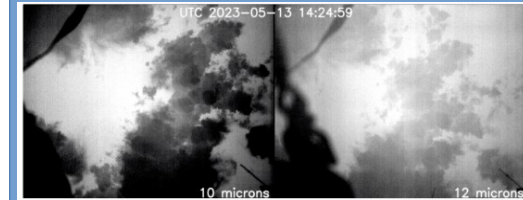
LF Radio Instrument

- Measures radio emissions from extensive air showers
- broadband 5 dBi gain from 50 MHz to 500 MHz in both V & H polarizations
- FoV: $60^\circ \times 120^\circ$



Infrared Camera

Quantifies cloud coverage within the telescope's FoV



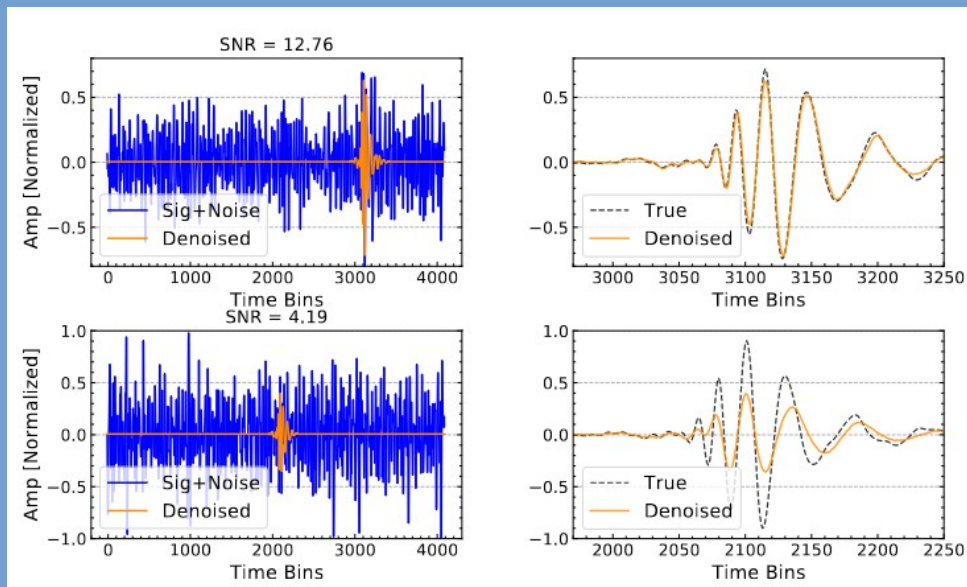
Gamma/X-ray/Particle

Measures the charged particle flux during flight and search for TLEs, TGFs, ToO events, and GRBs

Machine Learning Studies

ML with Radio

Radio signals of airshowers is very challenging due to only small signals compared to the background. **Uses CNNs to Denoise and Classify EAS emission signals from background noise**



A. Rehman, A. Coleman, F. G. Schröder, and D. Kostunin. Classification and Denoising of Cosmic-Ray Radio Signals using Deep Learning. PoS ICRC2021, 417, 2021.

Early Study EAS Reconstruction from Above using ML

Focuses on utilizing CNNs to reconstruct key parameters of EAS, such as geometry, energy, and X-max of EAS events by convolving a 4D (x pixel, y pixel, time, and photon count) into 3D (x pixel, y pixel, functional attributes).

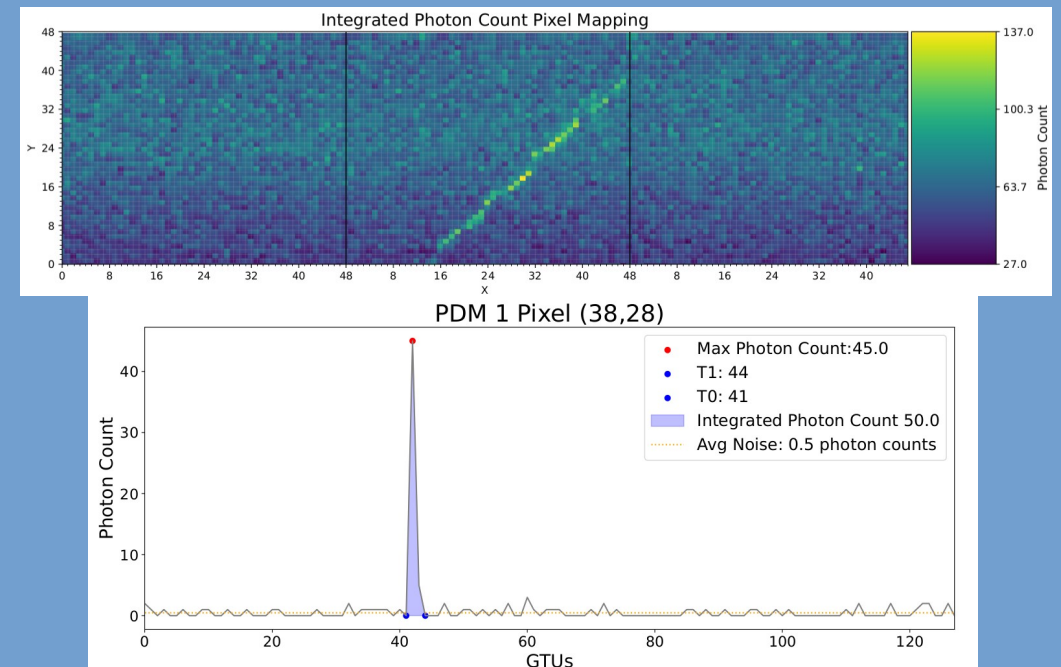


Photo-hadronic pair creation in magnetospheric current sheets of accreting black holes

Despina Karavola

National and Kapodistrian University of Athens

PhD Student

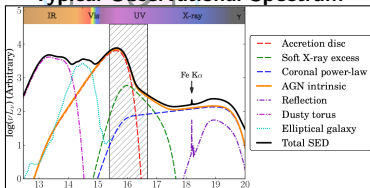
Cosmic-Ray International Studies and Multi-messenger Astroparticle
Conference
Trapani

June 2024

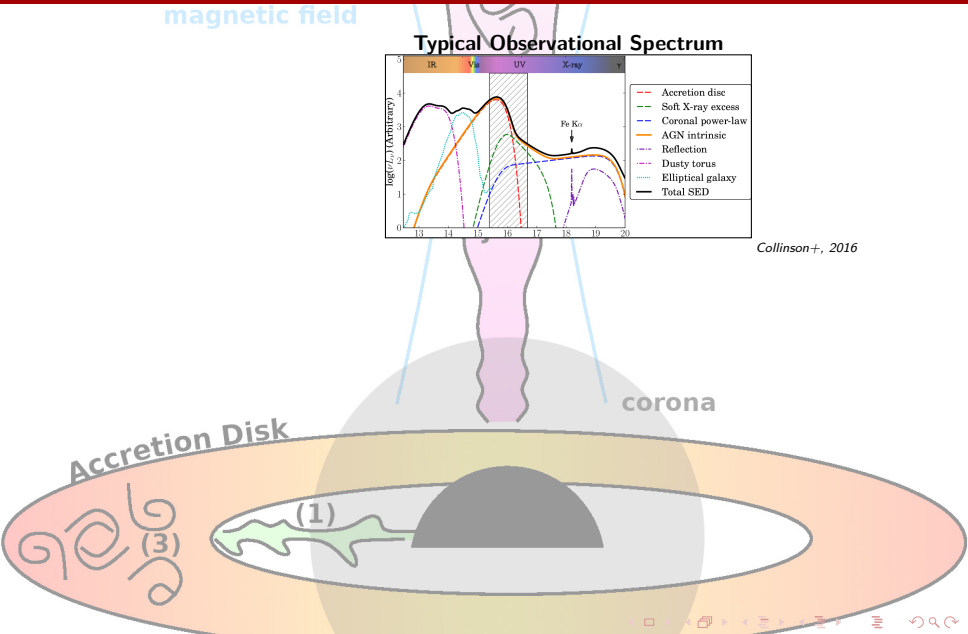
Simple X-Ray Corona Model

magnetic field

Typical Observational Spectrum



Collinson+, 2016



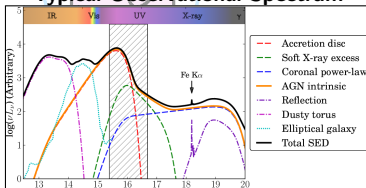
Simple X-Ray Corona Model

magnetic field

Numerical Leptohadronic Code Used:

ATHEνA

Typical Observational Spectrum



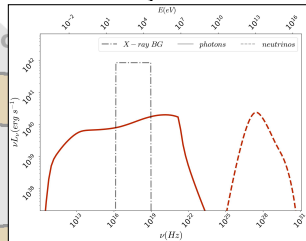
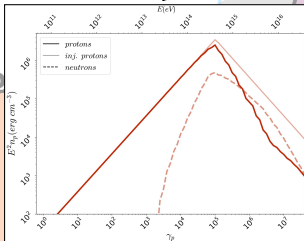
Collinson+, 2016

$$\sigma_p = \frac{B^2}{4\pi n_p \text{ cold } m_p c^2}$$

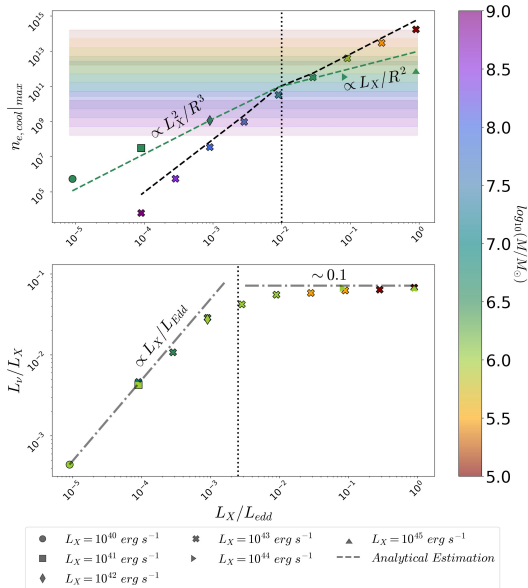
BPL p + energy dist.
w/ peak at $\gamma_p = \sigma_p$

PL X-ray photon dist.
 $E \in [100\text{eV}, 100\text{keV}]$

Accretio



What do we find?



- ➡ $L_X/L_{edd} \gtrsim 10^{-2} \Rightarrow$ sufficient pair density for a corona with $\tau \sim 0.1 - 10$
- ➡ $n_{e,cool} \propto L_X^2/R^3$ for optically thin sources to Thomson scattering
- ➡ $n_{e,cool} \propto L_X/R^2$ for opaque sources to Thomson scattering
- ➡ $L_V \propto L_X^2/L_{edd}$ for optically thin sources
- ➡ $L_V \propto L_X$ for opaque sources



Thank You!

Discovering cosmic rays: a link between education and research in a high school physics teachers' course



R. Antolini¹, C. Aramo², A. Candela¹, N. D'Ambrosio¹,
M. De Deo¹, A. Giampaoli¹, S. Hemmer³, A. Iuliano², I. Veronesi^{2,4}
for the OCRA Collaboration
¹INFN-LNGS, ²INFN-Napoli, ³ INFN-Padova, ⁴University of Salerno

Introduction

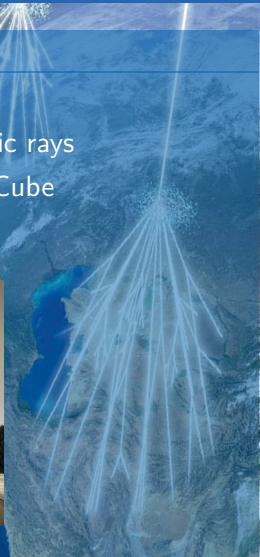
- **What:** a cosmic rays course for high school physics teachers
- **Who:** 17 teachers of physics from all Italy
- **When:** 11-13 December 2023
- **Where:** INFN Gran Sasso National Laboratories
- **How:** Lectures, Laboratory Activities, Real Data Analysis, Preparation of Teaching Pathways
- **CTA+ PNRR** Project (IR0000012; CUP C53C22000430006)



Lectures

Covered Topics

- Brief review of origin and physics of cosmic rays
- Layout and operation of the Cosmic Ray Cube
- Introduction to the laboratory activities



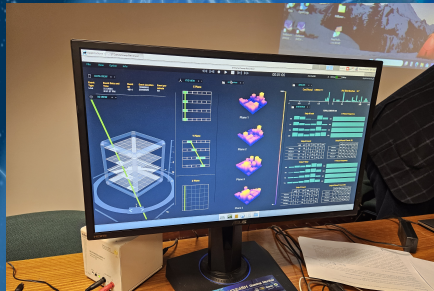
Construction of the Cosmic Ray Cube

- Plastic scintillator: 4 modules, 2 layers for XZ and YZ views
- Each layer is made of $24 \times 4 \times 1 \text{ cm}^3$ bars
- Receive kit of materials provided by the INFN
- Assembly of the detector bars of each plane
- Connection to the front-end electronic layout



Data Analysis

- Real-time access with the app “**Cosmic Ray Live**”
- Measurement of the muon intensity as a function of the angle formed with the local zenith
- Discussion of the results and comparison with the expected $\cos^2 \theta$ function



Teaching Pathways

- Divided into groups of two or three teachers
- Set up education activities with technology, laboratory work, experimentation, and teamwork
- Planning for the realization of the proposals

After the course:

- Cosmic Month in the classrooms
- Meeting for feedback from teachers
- Next edition: Padova, September 2024